

**Metal—Hydride Formation Mechanism
Measured by Acoustic Emission Methods**

Jiaxiang Piao

Doctoral Program in Advanced Materials Science and Technology

Graduate School of Science and Technology

Niigata University

August 2015

Abstract

Hydrogen storage alloys are important in the energy storage area because of that these alloys have the capacity to absorb and desorb amount of hydrogen. There are a lot of interests in the formation mechanism of metallic hydride. It has been known that the change of lattice energy of a transition metal by hydrogenation is interpreted in the terms of the lattice expansion and the change of Fermi level by our research group. In this thesis, we focus on the phenomenon of that metal transformed by slight stress in the case of hydrogenation easily and want to clarify the formation mechanism of metallic hydride. We will propose acoustic emission measurement methods by using gas pressure technique and electrochemical charging technique in order to obtain the dynamical information of hydrogenation process of palladium. The analysis with the experimental results was discussed by the dislocation theory.

This thesis includes 4 chapters.

In the first chapter, the motive and purpose of this research was stated.

In the second chapter, a hydrogenation process of palladium has been studied by acoustic emission (AE) methods with a new gas pressure cell. By using noble Ar gas, the AE events were observed intermittently for the stepwise pressurization. On the repetition of the re-pressurization, the AE events showed the Kaiser effect, *i.e.*, a dislocation motion induced effect. The typical power spectrum of AE signal by noble gas demonstrated the fundamental signal modes of 250 and 550 kHz. By the hydrogen gas re-pressurization, the characteristic AE behavior was recognized as following: 1) The continuous AE events were observed by the stepwise pressurization, 2) in the early stage of primary H solid solution of Pd, the fundamental AE modes were measured as 250 and 550 kHz, 3) in the hydride formation stage, the continuous AE events were also

observed, and the typical AE mode was changed to 250 kHz mainly. The hydride formation mechanism was discussed on the basis of the dislocation theory. From these results, when a hydrogen atom is dissolved into an fcc metallic lattice, it occupies an interstitial octahedral site and pushes aside metal atoms around its site as is recognized from the lattice expansion induced by hydrogenation.

In the third chapter, a hydrogenation process of Pd was studied by AE method with a new electrochemical hydrogen charging technique. The AE measurement method with the electrochemical separated AE cell by removing coexisted AE waves with generated H₂/O₂ gas on the counter electrode. Characteristic AE power spectra caused by cavitation and /or bubble burst have been appraised by using an electrochemical separated AE cell. The characteristic of the AE power spectrum due to Pd hydride formation was around 250 kHz. In the second chapter, the spectrum was evaluated as 250 kHz obtained using gas pressure AE cell. This means that the AE method with the electrochemical AE cell will be a powerful way to investigate the hydride formation mechanism because the high H₂ gas pressure condition can be easily provided by hydrogen over voltage.

In the forth chapter, we make a conclusion about this thesis. We established the validity of the AE measurement methods by using gas pressure technique and electrochemical charging one. And, we propose that the partial dislocation of Pd lattice will play an important role in hydride formation. Finally we will propose that this research could contribute to the research and development of, for instance, aluminum based hydride alloys which crystal structure will drastically change by hydrogenation.

Content

Chapter 1 Introductory Remarks

General Introduction.....	2
1.1 Background	2
1.2 Formation mechanism of metallic hydride	2
1.3 hydrogenation methods	3
1.4 Acoustic emission technique.....	4
1.4.1 History	4
1.4.2 Kaiser effect.....	5
1.4.3 AE Sensors.....	5

Chapter 2 Acoustic Emission Acoustic Emission Measurements on Palladium Hydrogenation Process by Using New Gas Pressure Cell

2.1. Introduction.....	7
2.2 Experimental section.....	8
Materials	8
Operating system.....	9
Experimental procedure.....	10
2.3 Results and Discussion.....	10
AE measurements by using standard Ar gas	10
AE measurements of the Pd hydrogenation process	14
2.4. Experimental Analyses and Discussions.....	18
2.5 Summary	22

Chapter 3 Acoustic Emission Measurements on Metal—Hydrogenation Process by Using Electrochemical Charging Cell

3.1. Introduction	25
3.2. Experimental procedure.....	26
3.3. Experimental Results and Evaluations	28
3.3.1 The preliminary experiments and results	28

3.3.2 Experimental results of O ₂ /H ₂ gas generated on working Pt electrode as basic data	30
O ₂ gas generated on Pt.....	30
H ₂ gas generated on Pt electrode	33
3.3.3 Experimental results on Pd electrode as present purpose	36
O ₂ gas generated on Pd electrode	36
AE measurement of Pd hydrogenation.....	39
3.4. Summary.....	42

Chapter 4 Conclusion

Conclusions	44
References	47
Acknowledgements	50
APPENDIXS	51
Appendix 1	52
Appendix 2	55
The relation of pressure p with chemical potential Φ	55

CHAPTER 1

INTRODUCTORY REMARKS

General Introduction

1.1 Background

In recent years, the concepts of saving energy, reducing pollution, protecting the environment, and developing long-term energy supply solutions were the main focus by the public attention.¹⁻⁴⁾ The world's current energy supply system which is mainly based on fossil fuels has become a matter of concern.⁵⁻¹³⁾ A widespread use of fossil fuels by a constantly growing world population (from 2.3 billion in 1939 to 6.5 billion in 2006) gives rise to the problem of oil supply. The problem related to the oil supply is caused by the fact that fossil fuels are not renewable primary energy sources. This means that since the first barrel of petroleum has pumped out from the ground, we have been exhausting a heritage given by nature.⁵⁻⁷⁾ The use of fossil fuels, such as petroleum, the remaining oil would be supplied of only about 40 years, if current demand remains static. As a consequence of the problem of energy supply, the world will have will have to reduce its fossil fuel consumption rate,²⁻³⁾ build more efficient and that consumes less power plants, use hybrid technology in the transportation sector. These may be non-conventional oil and gas, renewable energy (solar, hydro, wind, biomass), and nuclear energy. Nowadays, electricity is the most used energy carrier. The fuel cell, which is an electrochemical device that combines hydrogen fuel with oxygen, produces electric power, heat, and water only.^{5, 7, 10-13)} Therefore, the fuel cell technology and hydrogen as an alternative energy carrier are considered the ultimate goal of a secure energy supply and a clean environment. Unlike electricity, hydrogen can be stored for a long period of time in the hydrogen energy storage system.¹⁴⁻¹⁷⁾

1.2 Formation mechanism of metallic hydride

There are a lot of interests in the formation mechanism of metallic hydride. The

measurement of sound density is an experimental way in derivation of bulk modulus with lattice expansion by hydrogen concentration.¹⁸⁾ When a hydrogen atom is dissolved into an fcc metallic lattice, it occupies an interstitial octahedral (O) site and pushes aside metal atoms around its site as is recognized from the lattice expansion induced by hydrogenation.¹⁹⁾ In a case of palladium-hydrogen (Pd-H) system, the solubility of hydrogen, x , increases with increasing pressure of H₂ gas, p , at a given temperature as a function of the square-root of p .²⁰⁾ The dissolution and diffusion measurements show that the penetration time of H in Pd sheet of 140 μm is 67 s at 297 K.²¹⁾ The occupied spaces of H are the interstitial octahedral sites of Pd. The number of O sites in the fcc lattice is equal to that of the host Pd atom and palladium absorbs large amounts of hydrogen, up to $x = [\text{H}]/[\text{Pd}] = 1$,²²⁾ where the square brackets [B] means the number of B atoms. The concentration range of around $x < 0.01$ is called primary solid solution α phase, and $x > 0.6$ is hydride β phase at room temperature. Except for the regions is $\alpha+\beta$ two phases, *i.e.*, the spinodal decomposition region due to the long-range attractive H-H interaction. The volume expansion of the host lattice in the α to β transition is $\Delta V = 1.57$ cm³/g-atom of H.²³⁾ The free energy of Pd-H system has been measured by thermal analysis and/or electrochemical methods and the formation mechanism of Pd hydride was interpreted on the basis of the lattice relaxation energy and the change of Fermi energy.²⁴⁻²⁶⁾

1.3 hydrogenation methods

Generally there are two kinds of hydrogenation methods, the gas pressure method and the electrochemical charging method. During hydride formation, host lattice will expand with hydrogen concentration. That is, lattice distortion energy will be increased by

hydrogenation. Acoustic emission (AE) measurements are useful investigating method for dislocation motion caused by applied stress and/or lattice distortion. And the AE technique is a powerful method for the in situ analysis of physical phenomena induced by distortion energy.

The H₂ gas pressure method is a fundamental hydrogenation technique. In general, high H₂ gas pressure is required to form the hydride. On the other hand, electrochemical hydrogen charging technique is a powerful way of making the specimen absorbing hydrogen directly. The relation of pressure p with chemical potential Φ is given by equation of $p = p_0 \exp(2\Delta\Phi/kT)$, where p_0 is standard pressure, Φ : over potential, k : Boltzmann constant and T : temperature, as will be derived in appendix 1. In the case of $T=298$ K and $\Delta\Phi=0.1$ V, the equivalent H₂ gas pressure is 240 MPa, and $\Delta\Phi=0.15$ V gives 10 GPa at the same temperature.

1.4 Acoustic emission technique

1.4.1 History

The history of acoustic emission can be divided on two main periods: pre-technological and technological. From the beginning of humankind, people were observing acoustic emission when heard cracking stones, fracturing of bones, crackling of wood in the fire and so on. With development of work crafts, acoustic emission was helping craft makers to control quality of production. For example, during pottery making, cracking sounds were indications of fast or on-uniform pottery drying and this observation could be used for adjusting a process of pottery making.

The technological era of acoustic emission has started in the early 20th century when researches in different countries started to report about audible sounds during

investigation of material deformation. So in 1936, F. Forster and E. Scheil created and applied instrumentation for registration of AE generated during martensitic transformations.²⁶⁻²⁷⁾

1.4.2 Kaiser effect

In 1950, J. Kaiser investigating different engineering materials reported about the effect of the absence of acoustic emission in materials under stress levels below those previously applied on that material. This effect, bearing the name of Kaiser, is widely used in today's acoustic emission testing.

With development of the acoustic emission technology and the start of its extensive application, appeared a need in communication between researches, exchange of knowledge and common terminology. So for this purpose, starting from late 1960, there were organized acoustic emission working groups in USA, Germany, Japan and other countries. Also, there were developed standards for examination of structures, instrumentation and terminology. Today, acoustic emission testing is used practically in almost all industries and in many research centers.

1.4.3 AE Sensors

Acoustic emission sensor is a device that transforms a local dynamic material displacement produced by a stress wave to an electrical signal. AE sensors are typically piezoelectric sensors with elements made of special ceramic elements like lead zirconate titanate (PZT). These elements generate electric signals when mechanically strained. In this study, an AE sensor (PAC's WD of wideband differential type, TM of Physical Acoustic Corporation) is used, where the operating frequency range of the sensor is 100-1000 kHz with the resonant frequencies of 125 kHz and 650 kHz.

CHAPTER 2

Acoustic Emission Acoustic Emission Measurements on Palladium Hydrogenation Process by Using New Gas Pressure Cell

2.1. Introduction

There are a lot of interests in the formation mechanism of metallic hydride. In a case of palladium-hydrogen(Pd-H) system, the solubility of hydrogen, x , increases with increasing pressure of H_2 gas, p , at a given temperature as a function of the square-root of p .²⁸⁾ The dissolution and diffusion measurements show that the penetration time of H in Pd sheet of 140 μm is 67 s at 297 K.²⁹⁾ The occupied spaces of H are the interstitial octahedral (O) sites of Pd. The number of O sites in the fcc lattice is equal to that of the host Pd atom and palladium absorbs large amounts of hydrogen, up to $x = [\text{H}]/[\text{Pd}] = 1$,³⁰⁾ where the square brackets [B] means the number of B atoms. The concentration range of around $x < 0.01$ is called primary solid solution α phase, and $x > 0.6$ is hydride β phase at room temperature. Except for the regions is $\alpha+\beta$ two phases, *i.e.*, the spinodal decomposition region due to the long-range attractive H-H interaction.³⁾ The volume expansion of the host lattice in the α to β transition is $\Delta V = 1.57 \text{ cm}^3/\text{g-atom of H}$.³¹⁾ The free energy of Pd-H system has been measured by thermal analysis and/or electrochemical methods and the formation mechanism of Pd hydride was interpreted on the basis of the lattice relaxation energy and the change of Fermi energy.³²⁻³⁴⁾

Acoustic emission (AE) measurements are useful investing method for dislocation motion caused by applied stress and/or lattice distortion.³⁵⁻³⁷⁾ In this paper, we will propose an AE measurement method by using gas pressure technique in order to obtain the dynamical information of hydrogenation process of palladium.

2.2 Experimental section

Materials

A plate of Pd of 99.9 at. % purity was cold-rolled to a sheet of about 100 μm thick and annealed at 1173 K for 60 min in argon (Ar) 95 mol% and hydrogen (H_2) 5 mol% mixed gas. The sheet was cut into circular form of around 36 mm ϕ to set a gas pressure brassware cell shown in Fig. 2-1. The specimen sheet was clamped together at the roundness edges of the cell. Pressure gas was introduced from the left hand side in the figure. The “PG” in the figure means the pressure transducer (Copal Electronics; PA-830-103G) and the “PGA” is a simple pressure gage. The right hand chamber was safety zone for the specimen brittle fracture, where it was on an atmospheric pressure. Each AE sensor was a PAC’s model WD (TM of Physical Acoustics Corporation) with the operating frequency range of 100-1000 kHz and was arranged the opposite for localization measurements. The “TC” in the figure means thermocouple. The block diagram of AE measurement system is shown in Fig. 2-2.

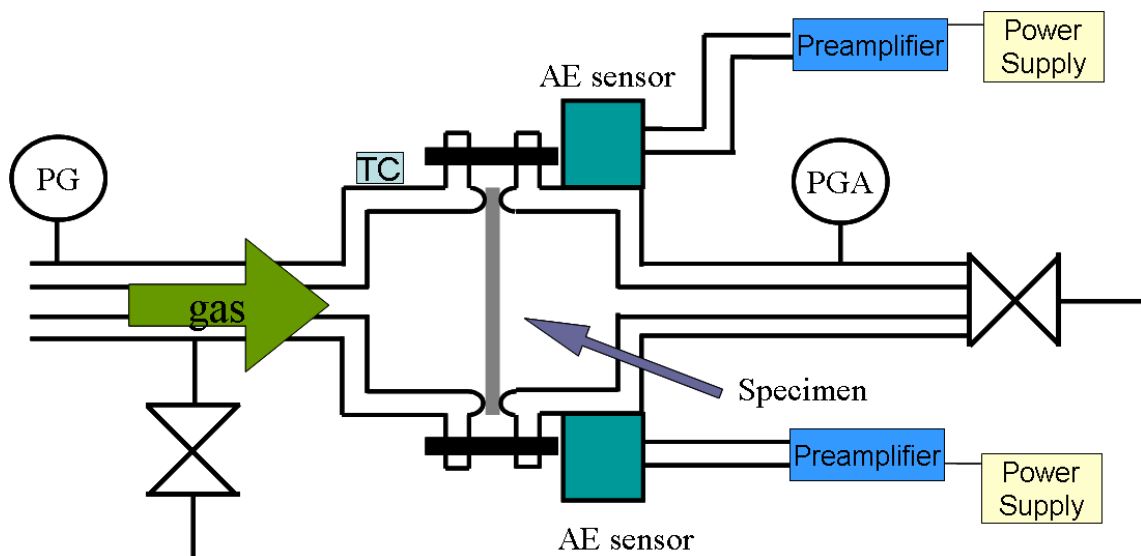


Fig. 2-1 Gas pressure AE measurement cell.

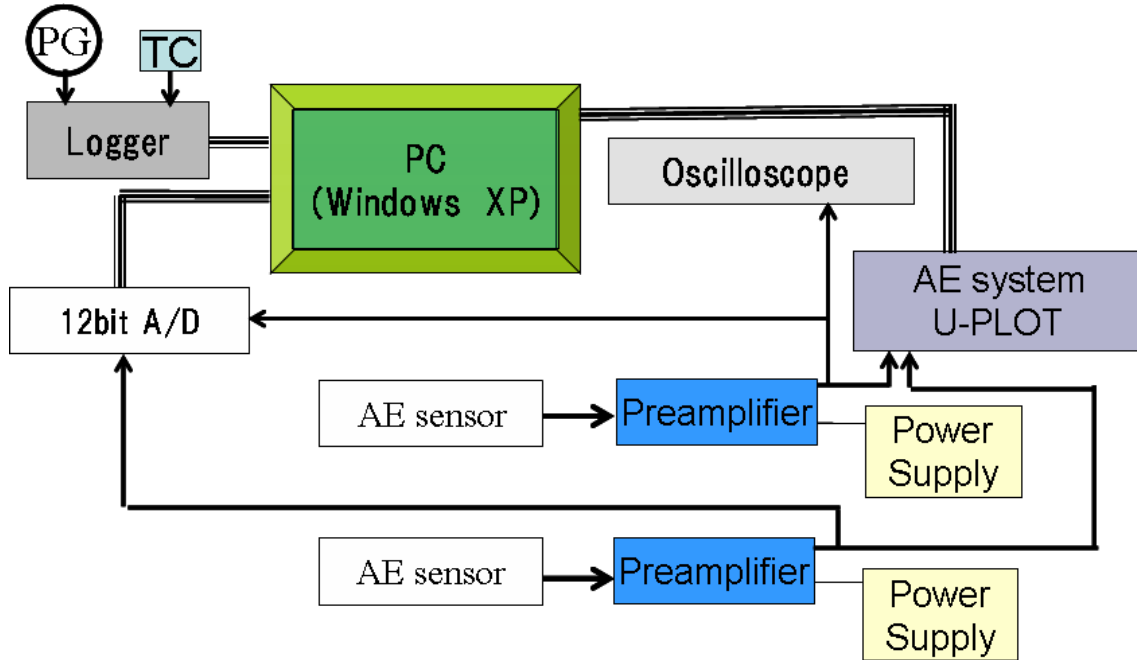


Fig. 2-2 Block diagram of AE system.

Operating system

The system was controlled by LabView (TM of National Instruments) language program. Each preamplifier was a PAC's 1220 (TM) with gain of 60 dB and a band-pass filter of 100-1200 kHz. The threshold value of U-Plot (TM of NF Electronic Instruments; 9502) of an AE analyzer was fixed at 63 dB for an AE event count level and a sampling trigger one, where the threshold level L of U-Plot is defined by $1 V = 100 \text{ dB}$, *i.e.*, $L(\text{dB}) = 20\log(V(\text{V}) \times 10^5)$. AE signals were captured by the trigger of U-Plot by using an analog input card (ADLINK Technology Inc.; NuDAQ PCI-9812) with the analog input resolution of 12-bit and the A/D sampling rate of 10 MHz. Their power spectrum was executed by using fast Fourier transformation (FFT) computation.

Experimental procedure

As a standard gas, Ar was used by using gas purge replacement method. Pressurization was performed from normal pressure of 0.1 MPa to 0.7 MPa by the 0.15 MPa with time interval of 600 s. After pressure-of-arrival of 0.7 MPa, re-pressurization was carried out with Ar gas through the same procedures from 0.1 to 0.7 MPa. After second arrival-pressurized by Ar, H₂ gas was introduced into the cell by gas purge replacement method at the normal pressure. And then, the pressurization by H₂ gas was executed from 0.1 MPa to 0.6 MPa by the 0.25 MPa and was kept constant at 0.6 MPa. A typical specimen forms before and after pressurization was shown in Fig. 2-3.

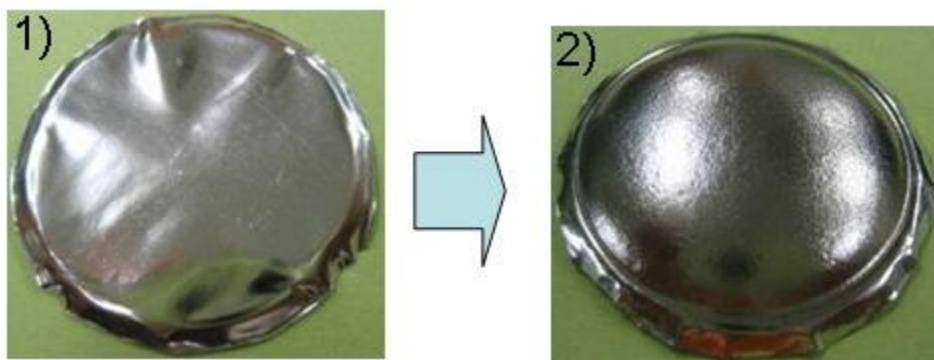


Fig. 2-3 Typical specimen form; 1) before and 2) after pressurization.

2.3 Results and Discussion

AE measurements by using standard Ar gas

Figure 2-4 shows typical AE signals of a Pd specimen by using Ar gas, where the choices of signals (1), (2) and (3) were done randomly at 600, 1200 and 1800 s, respectively. The beginning in a signal is noise. The threshold level at 63 dB of U-Plot corresponds to 0.014 V of the amplitude in the figure. The sampling interval of AE signal was 400 μ s from the sampling trigger and the pretrigger setting was 40 μ s.

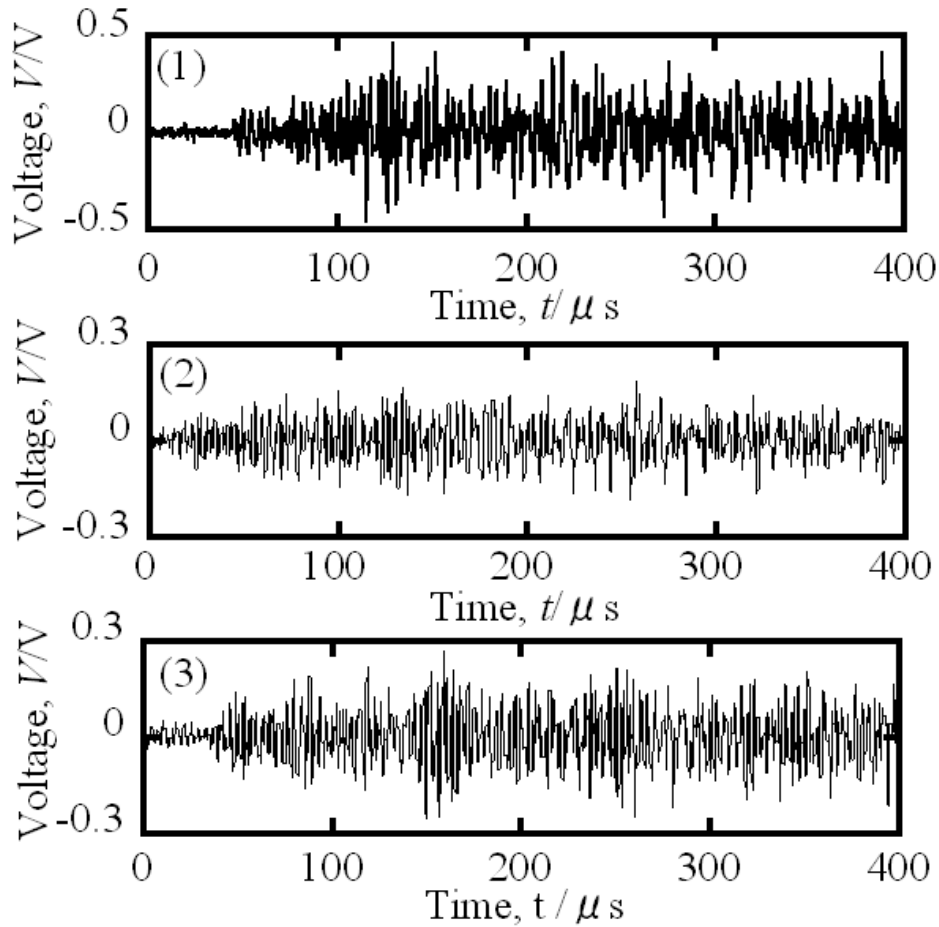


Fig. 2-4 Typical AE signals of Pd pressurized by Ar gas.

Figure 2-5 is typical AE power spectra of Pd pressurized by Ar gas. The spectrum (1) to (3) in the figure was the FFT spectrum of the AE signal (1) to (3) in Fig. 2-3, respectively. The data sheet of the AE sensor shows that the resonant frequency of WD is at 125 kHz and 650 kHz. Accordingly, the feature of the AE power spectra of the Pd pressurized by Ar gas was two intensity peaks around 250 kHz and 550 kHz. The intensity of two peaks were the same order on the average, and, their half width were around 100 kHz, respectively. The wide half width may be caused by various energies due to a burst of AE events.

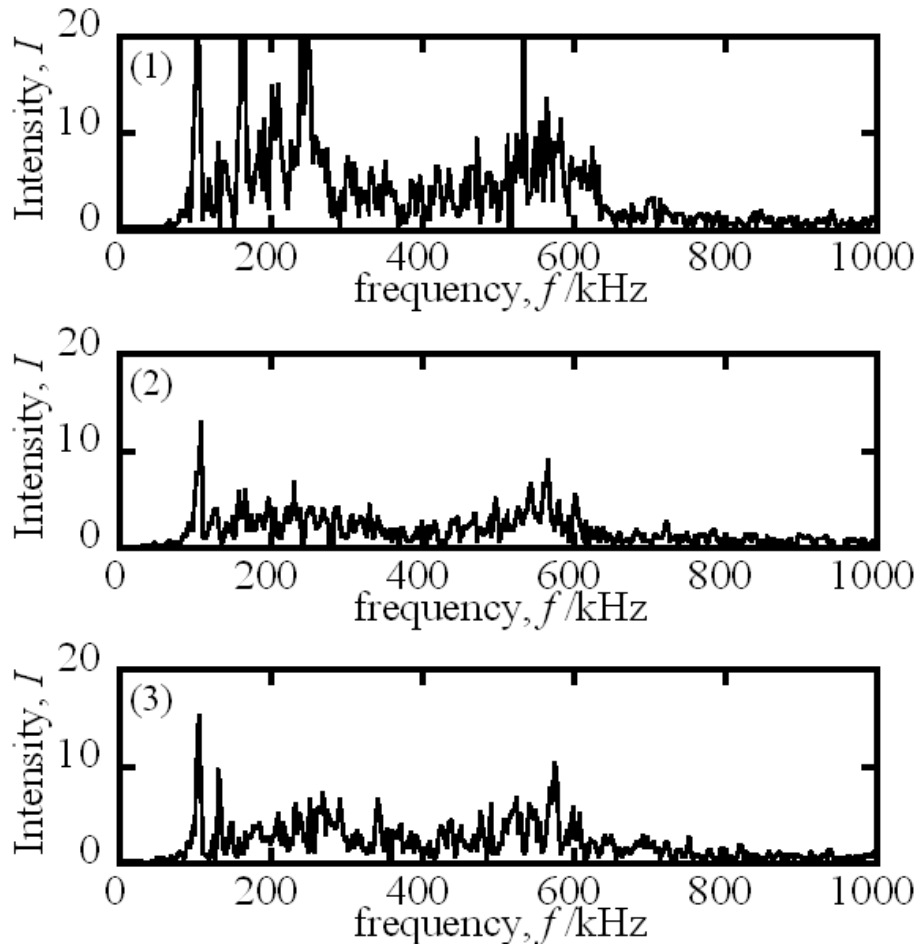


Fig. 2-5 Typical frequency spectra of Pd pressurized by Ar gas.

Figure 2-6 (1) shows the frequency of AE events per 1 s of the Pd on Ar pressuring process, *i.e.*, an AE events time histogram in a time interval of 1 s. The cumulative AE event counts are described in Fig. 2-6 (2). In the first step, pressurization was executed from the normal pressure of 0.1 MPa to 0.7 MPa. The AE events happened and concentrated at the times of the 600, 1200, 1800 and 2400 s just on the pressuring operation in a time interval of 1 s. After pressure-of-arrival of 0.7 MPa, second re-pressurization was carried out with Ar gas by the same procedures from 0.1 to 0.7 MPa. In the second step, AE events were not detected up to the 0.7 MPa as is

recognized in the figure. This phenomenon is known as the Kaiser effect. That is, the AE event has its maximum for an occurrence of distinctive yield strength, and accordingly, the AE is strongly influenced by inhomogeneous slip of the so-called slip dislocation.^{35, 36)} The total amount of event counts for the Pd sheet specimen using Ar gas was about 2500 counts under the present experimental conditions.

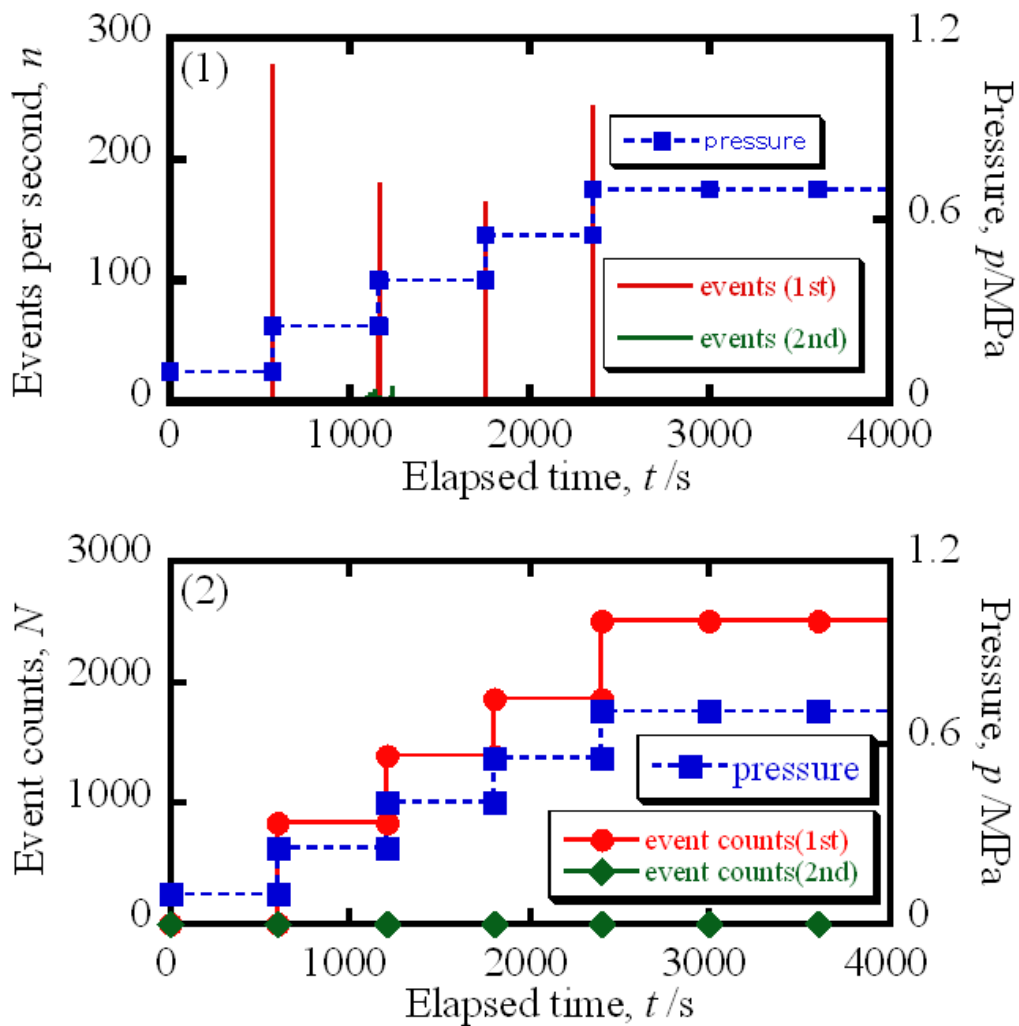


Fig. 2-6 AE events of Pd and the cell pressure by using Ar gas;

(1)frequency of AE events per second,(2)cumulative AE event counts.

AE measurements of the Pd hydrogenation process

The hydrogenation process of the Pd was investigated in on the Kaiser effect. That is, by using the Pd specimen which was pre-pressurized up to 0.7 MPa by Ar gas, none of the AE events will be expected to occur up to pressure-of-arrival of 0.7 MPa by the Kaiser effect. Figure 2-7 (1) and (2) show the frequency of AE events per 1 s and the cumulative AE event counts of the Pd pressurized by H₂ gas, respectively. This process was in the third step from the initial-pressurization by Ar. The H₂ gas pressurization was executed from the normal pressure of 0.1 MPa to 0.35 MPa at 600 s, and, was kept constant at 0.6 MPa after 1200 s. The experimental results on the event counts differ from those of Ar gas. The AE events in the hydrogenation process of Pd were happened “continually” even under the pressure-of-arrival. That is, this suggests a different AE generation mechanism on the palladium hydrogenation process. The total amount of event counts in the hydrogenation process of the Pd was around 300 counts, which was equal to about 1/10 of the applied stress by Ar gas.

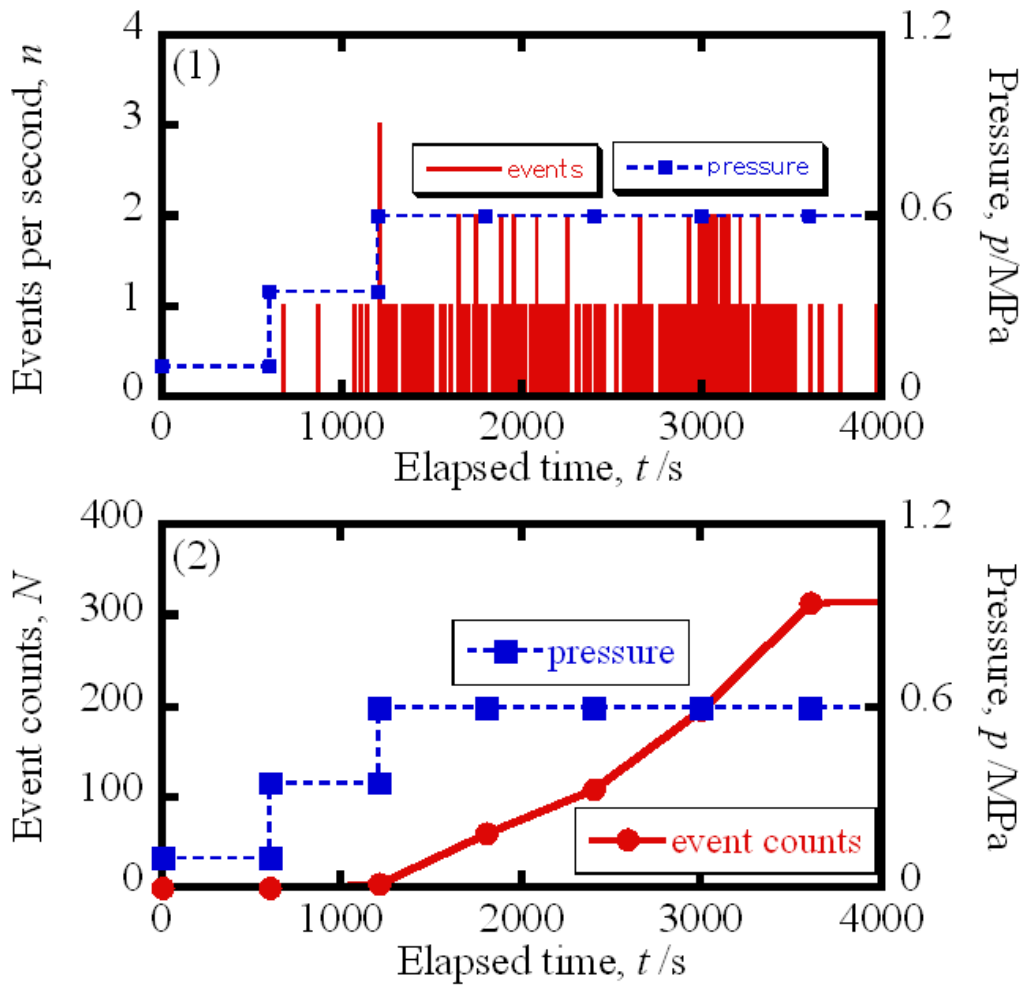


Fig. 2-7 Elapsed time dependence of AE events of Pd pressurized by H₂ gas; (1)frequency of AE events per second, (2)cumulative AE event counts.

In order to investigate the details of the hydrogenation process of the Pd, the x-ray diffraction(XRD) measurements were done at the 1800 s from stating the hydrogenation measurement and the 3600 s, where XRD measurements were done by using a specimen prepared by tracing method of the hydrogenation process of Pd. The XRD profile at 1800 s is given by Fig. 2-8(a). This profile means that the state of hydrogen in Pd was mainly in the α hydrogen solution phase. The amount of absorbed hydrogen was

evaluated as around $[H]/[Pd] = 0.1$.³²⁾ The other profile at 3600 s is given by Fig. 2-8 (b). This profile means that the hydrogen situation in Pd was in the β hydride phase. The amount of absorbed hydrogen was evaluated as around $[H]/[Pd] = 0.6$.³²⁾

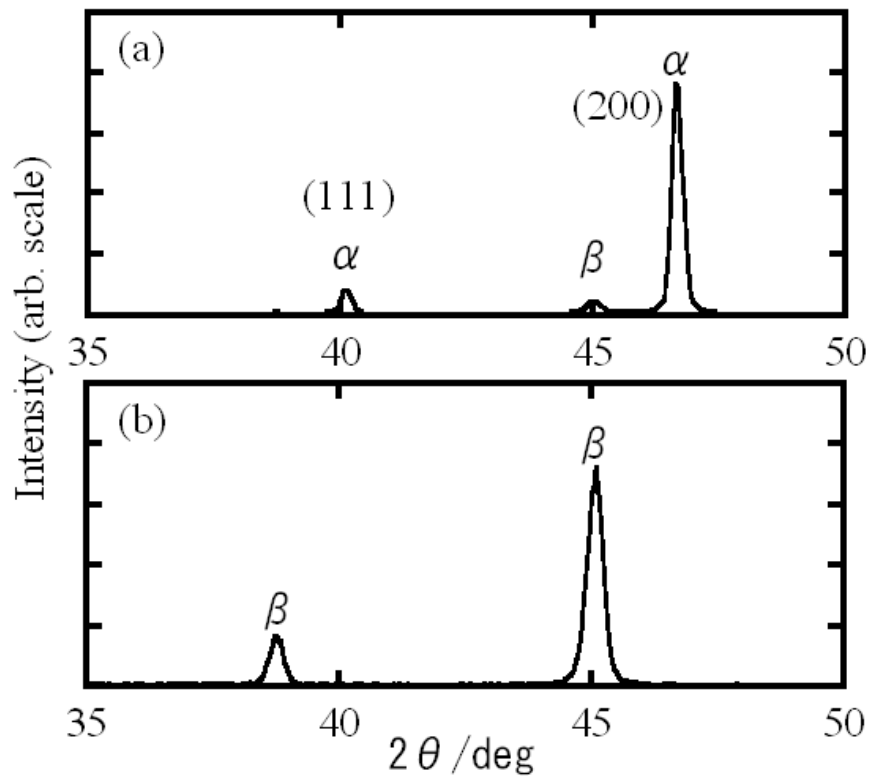


Fig. 2-8 X-ray diffraction profiles of hydrogenated Pd by using Cu $K\alpha$, (a)Hydrogenated Pd at 1800 s from starting the hydrogenation measurement, (b)Hydrogenated Pd at 3600 s, where α and β mean the hydrogen solution and hydride phases.

Typical AE power spectra of the hydrogenation process of the Pd around at 1800 s in Fig. 2-9, where the AE signals are shown in Fig.A1 in appendix 1. The power spectrum (4) to (6) in the figure correspond to the AE signal (4) to (6) in Fig. A1. The feature of

the AE power spectra of the Pd pressurized by H₂ gas was the intensity peaks around 250 kHz and 550 kHz, and, each intensity of two peaks were the same order on the average, and, their half width were around 100 kHz, respectively. Figure 2-10 is typical AE power spectra of the hydrogenation process of the Pd around at 3600 s, where the AE signals are shown in Fig.A2 in appendix 1. The power spectrum (7) to (9) in the figure correspond to the AE signal (7) to (9) in Fig. A2. The feature of the AE power spectra around at 3600 s was the intensity peaks was mainly 250 kHz with a narrow half width of around 20 kHz. This narrow half width suggests a simple AE event process.

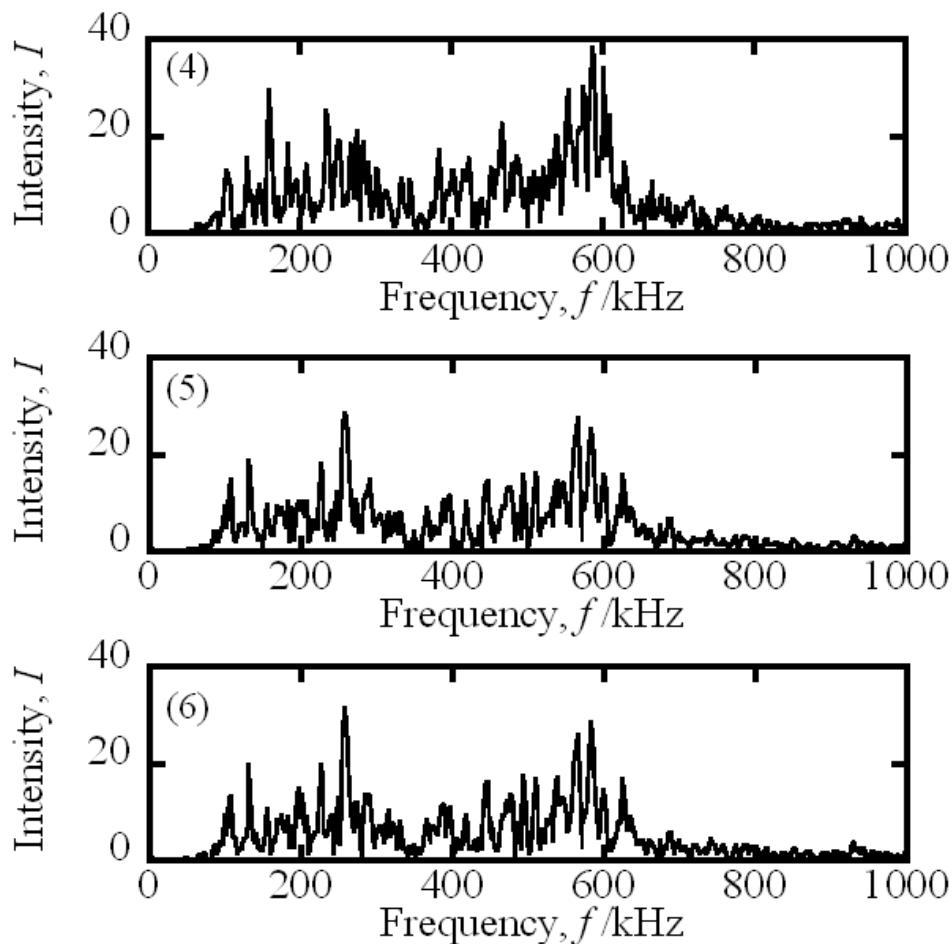


Fig. 2-9 Power spectrum of hydrogenation process of Pd at 1800 s from starting the hydrogenation measurement.

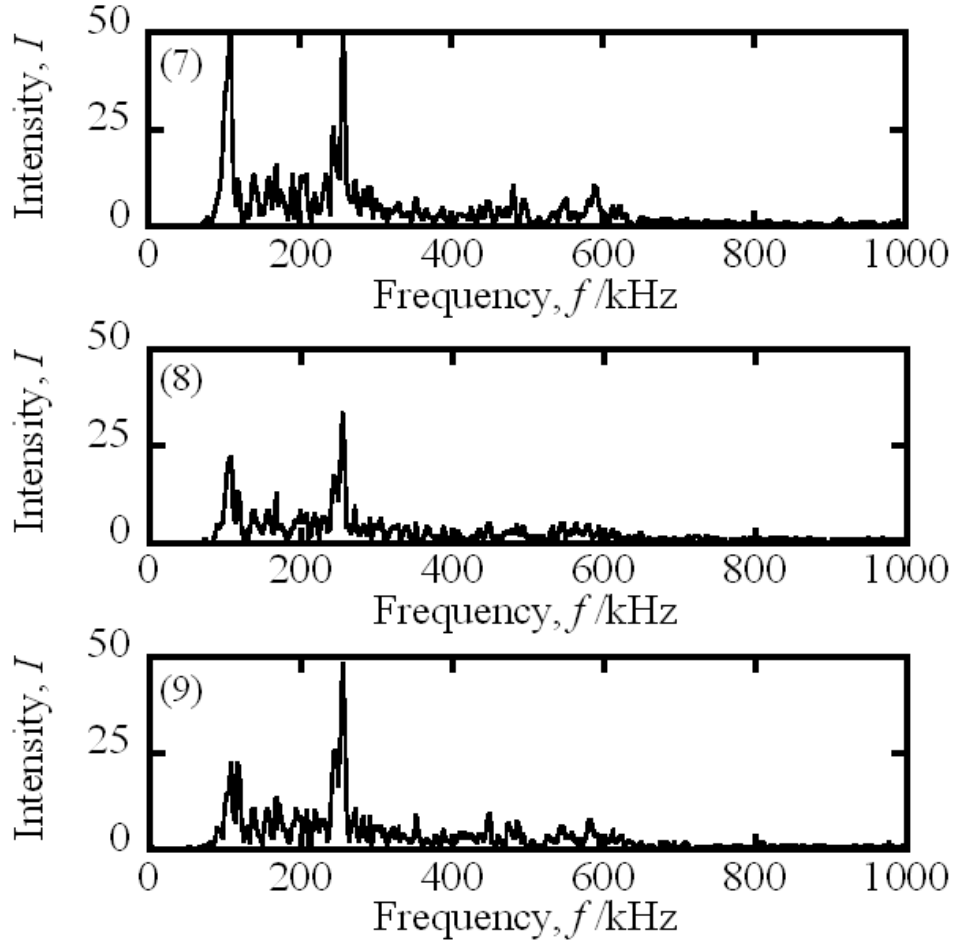


Fig. 2-10 Power spectrum of Pd signal at 3600 s from starting measurement.

2.4. Experimental Analyses and Discussions

The Kaiser effect revealed that the AE is induced by inhomogeneous slip of the slip dislocation.^{35, 36)} In order to evaluate the slip dislocation energy, we will introduce perfect dislocation and partial dislocation caused in fcc metal. The slip dislocation energy U is given by

$$U \approx \frac{Gb^2}{2} \quad (1)$$

in an approximate form. In this equation G is shear modulus, and b means the Burgers

vector. The Burgers vector of the fcc perfect dislocation for the slip direction $\langle 110 \rangle$ is

$$b^{\text{perfect}} = \frac{a}{2}(1, -1, 0), \quad (2)$$

where a means the lattice constant.³⁸⁾ That of the partial dislocation is given by

$$b^{\text{partial}} = \frac{a}{6}(1, -2, 1). \quad (3)$$

Accordingly, the ratio of partial dislocation energy to perfect one is rewritten as

$$U^{\text{partial}} : U^{\text{perfect}} = 1 : 3, \quad (4)$$

that is, $U^{\text{partial}} = (G/2)(a/6)^2(1 + (-2)^2 + 1)$ and $U^{\text{perfect}} = (G/2)(a/2)^2(1 + (-1)^2)$.

The above result will advise about the AE generation mechanism of Pd. In the AE generation mechanism by using standard Ar gas, the AE frequency peak around 250 kHz and 550 kHz as was shown in Fig. 2-4 should be due to the partial dislocation and perfect one, respectively. The normalized intensity of I_{250}^{aver} is 0.51 and that of I_{550}^{aver} is 0.49 in each subtotal width of ± 100 kHz, that is, was subtotal intensity of full width from 150 to 350 kHz of the (1) to (3) power spectrum and that of I_{550}^{aver} was that from 450 to 650 kHz of the same frequency range. The intensity ratio should be suggesting the frequency ratio of the partial slip dislocation and the perfect one. However, the influence of the sensitivity of the sensor, the wave propagation in the cell and the like did not take into account in this evaluation. The AE generation mechanism of the hydrogenation process of Pd has different ways from the dislocation motion caused by applied stress and/or lattice distortion pressurized by Ar. That is, the AE events in the hydrogenation process of Pd were induced “continually” as was shown in Fig. 2-7. The AE power spectra as was shown in Figs. 2-9 and 2-10 changes drastically within the hydrogenation process. In the α hydrogen solution phase at the 1800 s starting from the measurement, the normalized intensity of is 0.48 and that of I_{550}^{aver} is 0.52 in each

subtotal width of ± 100 kHz for the (4) to (6) power spectrum. In the β hydride phase at the 3600 s, has been increasing to 0.75 and I_{550}^{aver} is 0.25 in each subtotal width of ± 40 kHz for the (7) to (9) power spectrum. These experimental results will indicate the dynamical mechanism of hydride formation of Pd-H system. In order to investigate the details of the slip dislocation induced by the hydrogen, we have tested the outgassing process by using the AE method. The hydrogen gas was replaced by the normal pressure Ar by purging method. That is, the hydrogenated Pd with 0.6 MPa H_2 gas was decompressed to the normal pressure by using Ar gas purge replacement method, where the outgassing process of Pd hydride under various atmospheric conditions has been reported as a function of elapsed time by gravimetric method in a previous paper.³⁹⁾ The previous results showed that the hydrogen outgassing process of Pd was suppressed in a noble gas. Figure 2-11 shows the AE events time histogram of the outgassing process from the Pd- $\text{H}_{0.6}$ system in a time interval of 100 min. The event frequency was a little rare. The total amount of event counts in the outgassing process from the Pd- $\text{H}_{0.6}$ system was very few and was equal to about 1/10 of the hydrogenation process of Pd, where the AE measurement condition of the threshold value was 63dB. The AE signal turned to a weak and short wave-packet's signal, for instance, after 30 min from the stating of the outgassing process. Figure 2-12 shows typical AE power spectra in the outgassing process from the Pd- $\text{H}_{0.6}$ system at 6, 91 and 1180 min from the stating at the normal pressure of 0.1 MPa of Ar purge replacement environment. The feature of the AE power spectra of the hydrogen outgassing process seems to be contrary course of the hydrogenated one, that is, the intensity peak of 250 kHz turned to that of both 250 and 550 kHz.

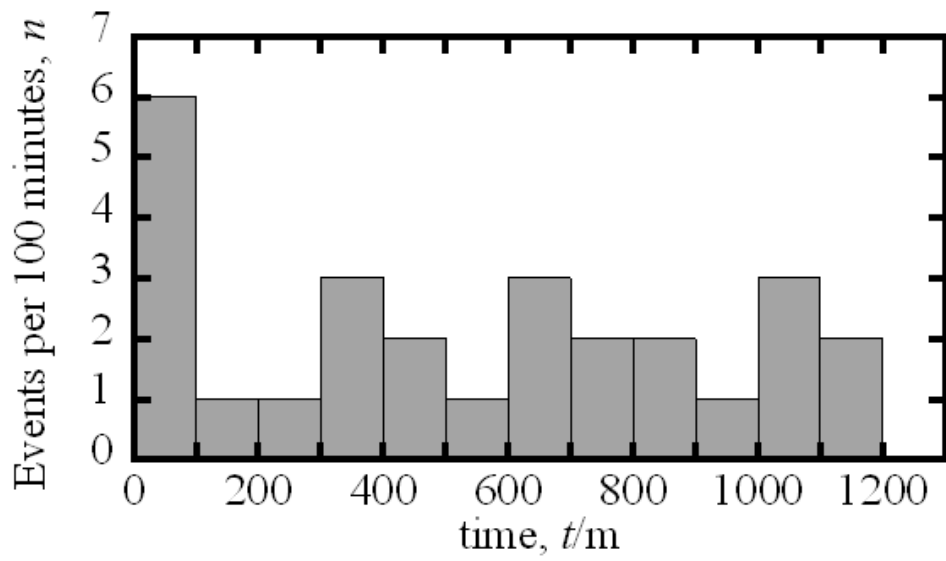


Fig. 2-11 AE events time histogram of the outgassing process from the Pd-H0.6 system.

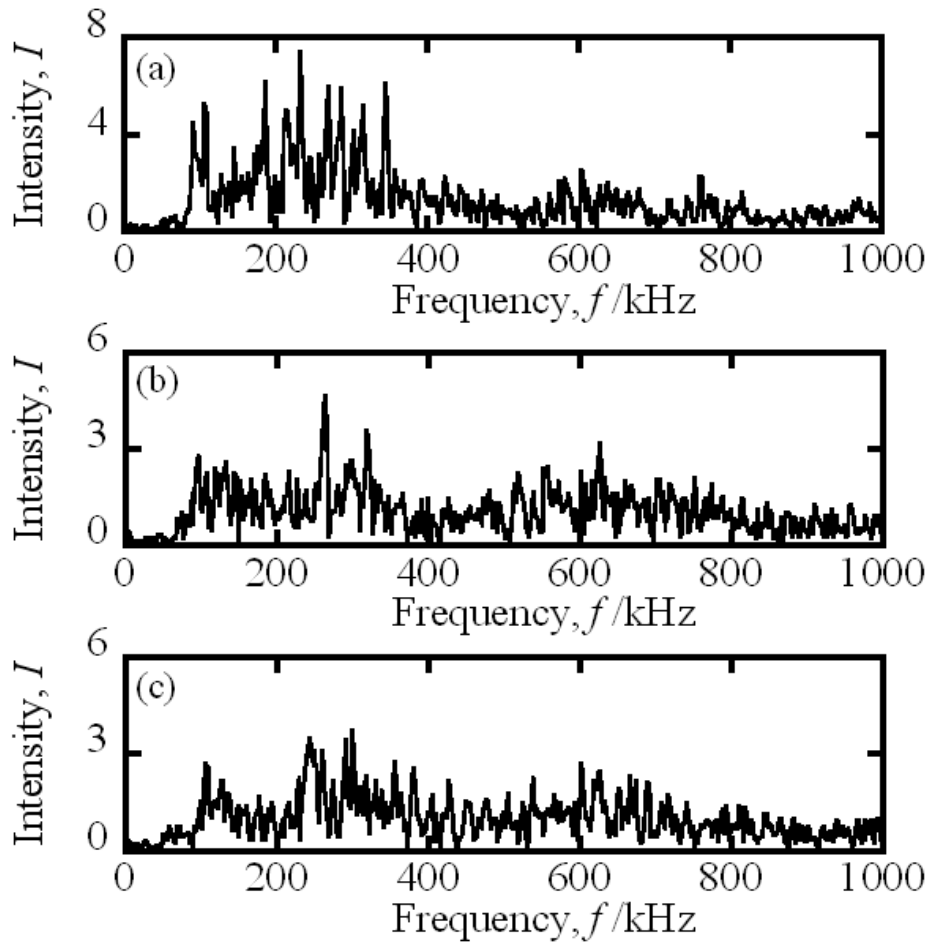


Fig. 2-12 Typical AE power spectra in the outgassing process of Pd-H system, (a) at 6 m, (b) 91 m and (c) 1180 m from the stating at the normal pressure of 0.1 MPa of Ar by purging method.

2.5 Summary

The AE events were observed by using a new gas pressure cell. The experimental results by Ar gas pressurization showed as following: 1) AE events happened just at the times of pressurization as was shown in Fig. 2-6, 2) the Kaiser effect was recognized in the re-pressurization process as was shown in Fig. 2-6, 3) the power spectrum of AE signal by noble gas showed the fundamental signals of 250 kHz and 550 kHz in Fig. 5,

4) the intensity of the power spectrum $I_{aver250}$ was 0.51 and that of $I_{aver550}$ was 0.49 in Fig. 5.

In order to investigate the details of the hydrogenation process of Pd, the AE events were observed by H₂ re-pressurization of the third pressuring process. The experimental results were different from those of Ar gas as following: 5) The AE events in the hydrogenation process of Pd happened "continually" as was shown in Fig. 2-7, 6) the total amount of event counts in the hydrogenation process by H₂ gas was equal to about 1/10 of the applied stress by Ar, 7) in the early stage of primary H solid solution of Pd, the intensity of the power spectrum I_{250}^{aver} was 0.48 and that of I_{550}^{aver} was 0.52, 8) in the hydride formation stage, the I_{250}^{aver} was increasing to 0.75 and I_{550}^{aver} was 0.25.

The slip dislocation energy of partial and perfect is evaluated by $U^{partial} : U^{perfect} = 1 : 3$ indicate that the AE 250 kHz and 550 kHz should depend on the partial dislocation and perfect one, respectively. Accordingly, we may propose the dynamical hydride formation mechanism with partial dislocation of Pd lattice.

CHAPTER 3

Acoustic Emission Measurements on Metal—Hydrogenation Process by Using Electrochemical Charging Cell

3.1. Introduction

Hydrogen storage alloys absorb a lot of hydrogen while forming metallic hydride. Generally there are two kinds of hydrogenation methods, the gas pressure method³⁸⁾ and the electrochemical charging method³⁹⁻⁴¹⁾. During hydride formation, host lattice will expand with hydrogen concentration. That is, lattice distortion energy will be increased by hydrogenation^{18-19, 42)}. The acoustic emission (AE) technique is a powerful method for the in situ analysis of physical phenomena induced by distortion energy⁴³⁻⁴⁴⁾. In a previous paper, we reported the hydrogenation process of palladium (Pd) by AE method with the gas pressure AE cell³⁸⁾. Through supplying noble Ar gas to the cell, the AE events of Pd sheet were observed intermittently during stepwise pressurization. On the repetition of three-pressurization of Ar gas, the AE events revealed the Kaiser effect, *i.e.*, a dislocation induced effect. The typical power spectrum of AE signal by Ar gas demonstrated the fundamental signal modes of 250 and 550 kHz. On the other hand, by the H₂ gas re-pressurization, the characteristic AE behavior was recognized as following: 1) The continuous AE events were observed by stepwise pressurization of H₂ gas, 2) in the early stage of primary H solid solution of Pd, the fundamental AE power spectra were measured as 250 and 550 kHz, 3) in the hydride formation stage, the continuous AE events were also observed, but the typical AE power spectrum shifted to 250 kHz mainly. These experimental behaviors were explained on the basis of the partial dislocation induced by Pd hydride formation³⁸⁾.

The H₂ gas pressure method is a fundamental hydrogenation technique. In general, high H₂ gas pressure is required to form the hydride. On the other hand, electrochemical hydrogen charging technique is a powerful way of making the specimen absorbing hydrogen directly. The relation of pressure p with chemical potential Φ is given by

equation of $p = p_0 \exp(2 \Delta \Phi / kT)$, where p_0 is standard pressure, Φ : over potential, k : Boltzmann constant and T : temperature, as will be derived in appendix. In the case of $T=298$ K and $\Delta \Phi=0.1$ V, the equivalent H_2 gas pressure is 240 MPa, and $\Delta \Phi=0.15$ V gives 10 GPa at the same temperature⁴⁵⁾.

In this paper, we propose an AE measurement method with the electrochemical separated AE cell by removing coexisted AE waves with generated H_2/O_2 gas on the counter electrode⁴⁶⁾. We chose Pt as non-absorbable H specimen⁴⁵⁻⁴⁶⁾ and Pd as absorbable H⁴⁷⁻⁴⁸⁾. We established the validity of the AE measurement method with the electrochemical technique in accordance with the standard gas pressure hydrogenation technique.

3.2. Experimental procedure

A plate of Pt and Pd of 99.95 at. % purity was cold-rolled to a sheet of 100 μm , and annealed at 1173 K for 1h in Ar 95 mol% and H_2 5 mol% mixed gas. The sheet was cut into circular form of around 18 mm Φ to be settled on the surface of AE sensor with slight grease mechanically.

Figure 3-1 shows the electrochemical separated AE cell. Electrolytic bridge was used to avoid the coexisted AE waves with generated H_2/O_2 gas on the counter electrode (CE). The circular sheet was used for the working electrode (WE). The effective surface area of WE was $1.00 \times 10^{-4} \text{ m}^2$. The CE was made of rectangular Pt sheet with effective surface area of $1.00 \times 10^{-4} \text{ m}^2$. The electrolyte is the H_2SO_4 solution of 0.05 mol/L. In the Fig. 3-1, PC means personal computer, and the system was controlled by LabView (TM of National Instruments) language program. The preamplifier was a PAC's 1220 (TM of Physical Acoustic Corporation) with gain of 60 dB. U-Plot (TM of NF

Electronic Instruments; 9502) is the AE analyzer. The sampling interval of AE signal of U-Plot was 400 μ s from the sampling trigger and the pretrigger setting was 40 μ s. The time data of U-Plot was stamped on AE events with 1 s interval. The threshold level L of U-Plot was fixed at 63 dB for an AE event count level and a sampling trigger one, where L is defined by L (dB) = $20 \log (V (V) \times 10^5)$, *i.e.* 63 dB = 0.014 V. This threshold level was tested to avoid the electric noise and in order to obtain the adequate AE event counts. AE signals were captured by the trigger of U-Plot by using a 12-bit A/D card (ADLINK Technology Inc.; NuDAQ PCI-9812) with the A/D sampling rate of 10 MHz. Their power spectra were executed by using fast Fourier transformation (FFT) computation. An AE sensor (PAC's WD of wideband differential type, TM of Physical Acoustic Corporation) is settled with WE specimen, where the operating frequency range of the sensor is 100-1000 kHz with the resonant frequencies of 125 kHz and 650 kHz. In this paper, the power spectrum data was cut off from 800 kHz to 1000 kHz because of no useful information.

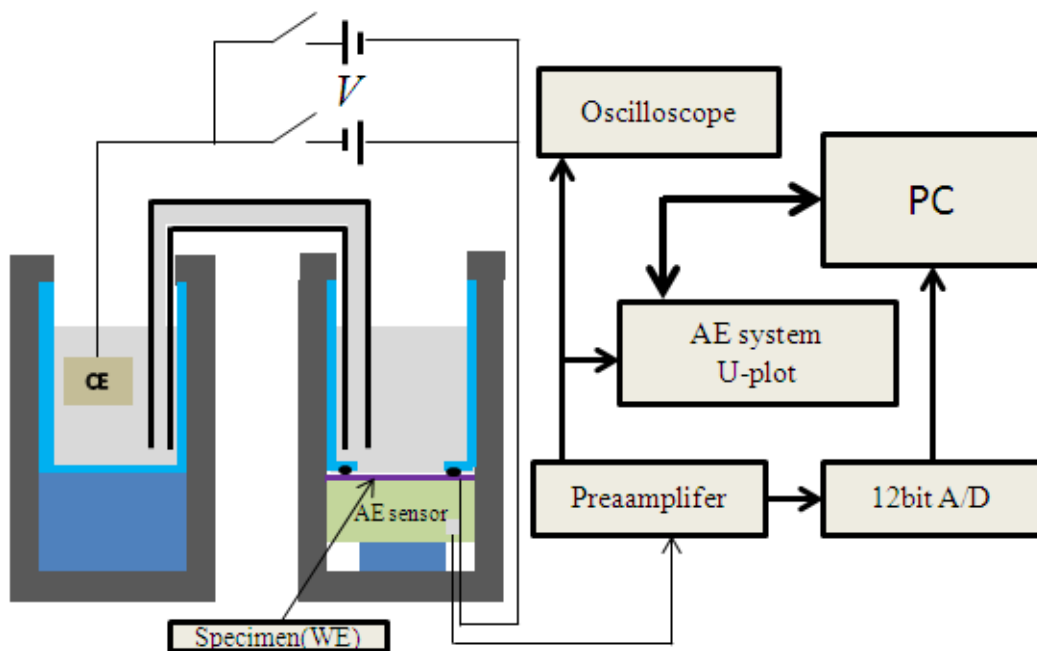


Fig. 3-1 Electrochemical AE measurement cell.

3.3. Experimental Results and Evaluations

3.3.1 The preliminary experiments and results

The preliminary experiments were done by using a testing AE cell as shown in Fig. 3-2. There was no AE signal during the electrolysis by using the AE cell (a). This means that the electrolytic bridge is a good attenuator to remove AE signals by generated H_2/O_2 gas on the electrodes and the propagated AE events will be negligible. Figure 3-2 (b) shows AE events for cavitations by generated O_2 or H_2 gas on Pt electrode E1. Figure 3-3 (a) and (b) show the results of generated O_2 and H_2 gas as a function of decomposition voltage from 3.0 to 5.5 V by stepping 0.5 V with a time interval of 10 min, respectively. This result suggests that AE signals induced by cavitations were attenuated in the electrolyte. The power spectra of the AE signals of O_2 and H_2 gas generated on Pt electrode were shown in Fig. 3-4 (a) and (b), respectively. The spectrum feature is an intensity peak around 280 kHz.

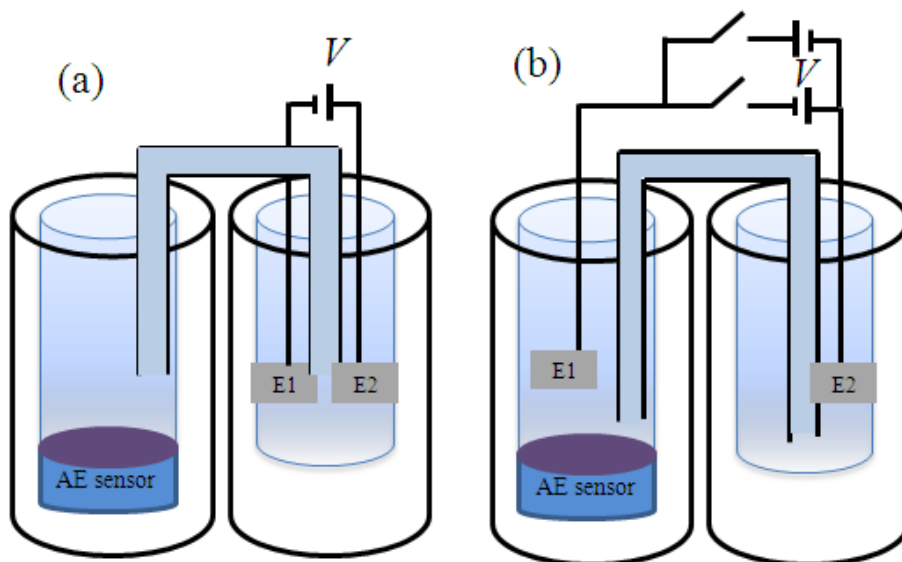
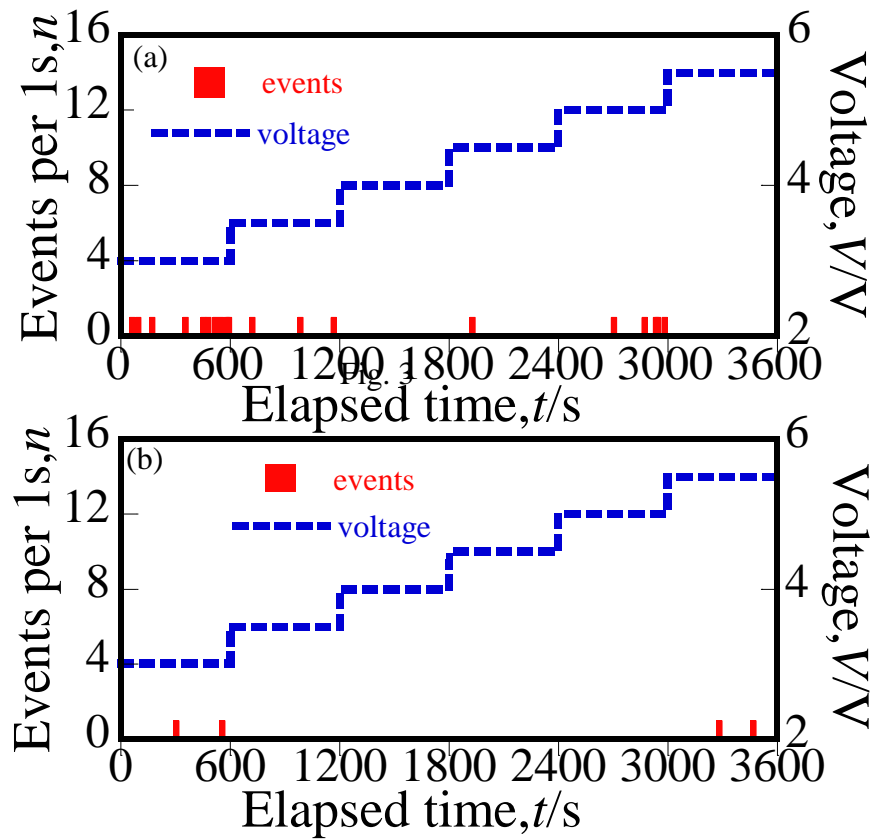
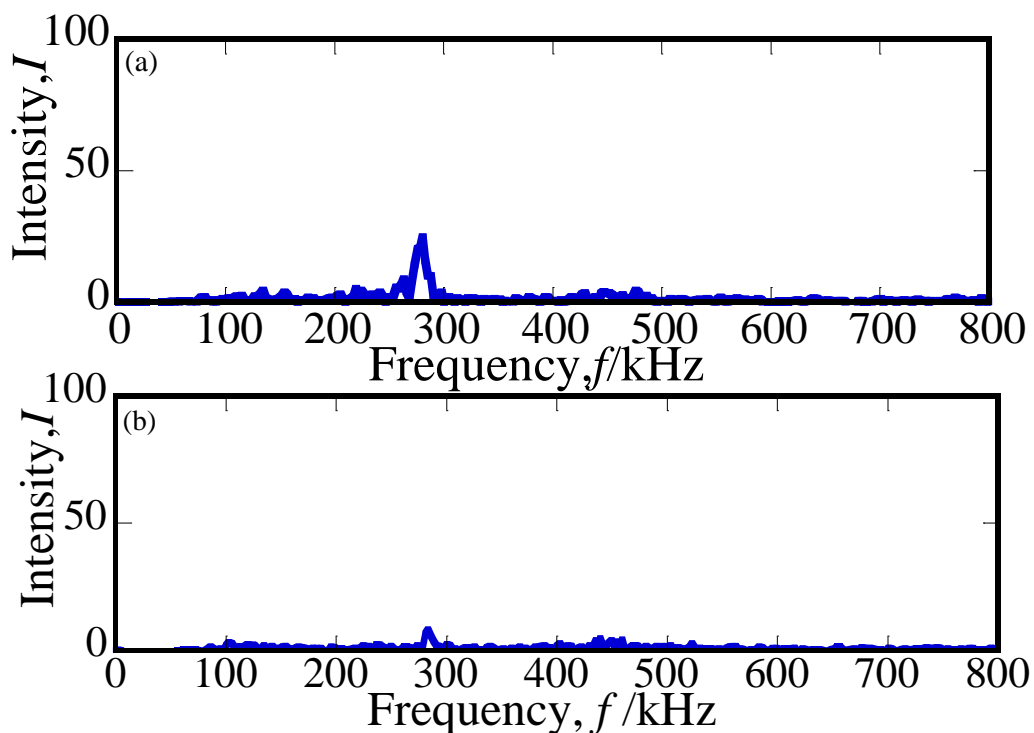


Fig. 3-2 Testing electrochemical cell.



**Fig. 3-3 AE events per second on Pt surface as function of decomposition voltage;
 (a)O₂ gas generated on Pt, (b)H₂ gas generated on Pt.**



**Fig. 3-4 Typical power spectrum of O₂ and H₂ gas generated on Pt electrode;
(a)O₂ gas generated on Pt, (b)H₂ gas generated on Pt.**

3.3.2 Experimental results of O₂/H₂ gas generated on working Pt electrode as basic data

O₂ gas generated on Pt

Figure 3-5 (a) shows AE events histogram per 1 s as a function of decomposition voltage by using electrochemical AE measurement cell as was shown in Fig. 3-1. To understand the oftenness of AE events generation as a differential form, the time interval is the maximum resolution of 1 s. The cumulative AE event is described in Fig. 3-5 (b) as an integral form. Figure 3-5 (c) shows current density versus applied decomposition voltage V . As an experimental relation, N was expressed by cubic polynomial of V . By using the same specimen, AE events behavior was the same in the re-applied of voltage, and in proportion to current density, that is, to the amount of O₂ gas generated on the working Pt electrode.

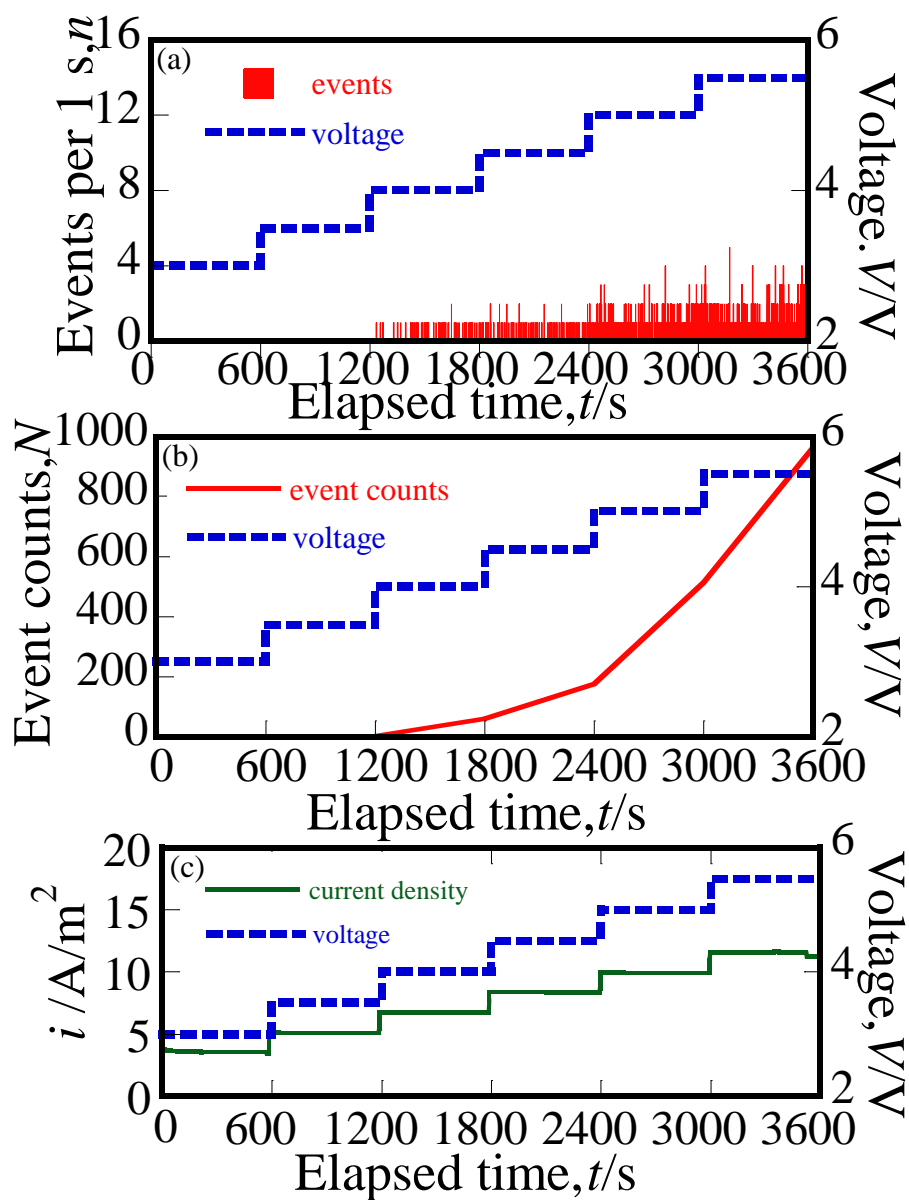


Fig. 3-5 AE events by O₂ gas generated working Pt electrode as a function of decomposition voltage;
(a) AE events per 1s, (b) cumulative AE event counts, (c) current density.

Figure 3-6 (a) and (b) show the typical of AE signals by O₂ gas generated on Pt electrode, which were randomly chosen. Figure 3-7 (a) and (b) are the FFT spectrum of the corresponding signals, where the observed oftenness was around 92 % and 8 %, and the observed intensity at 280 kHz peak was 50 and 200, respectively. Accordingly, the feature of the AE power spectra of O₂ gas generated on Pt was 280 kHz induced by cavitation, where the power spectra of 125 kHz and 650 kHz are due to the resonant frequencies of the WD AE sensor. The origin of the power spectrum (b) may be induced to O₂ bubble burst by watching the decomposition.

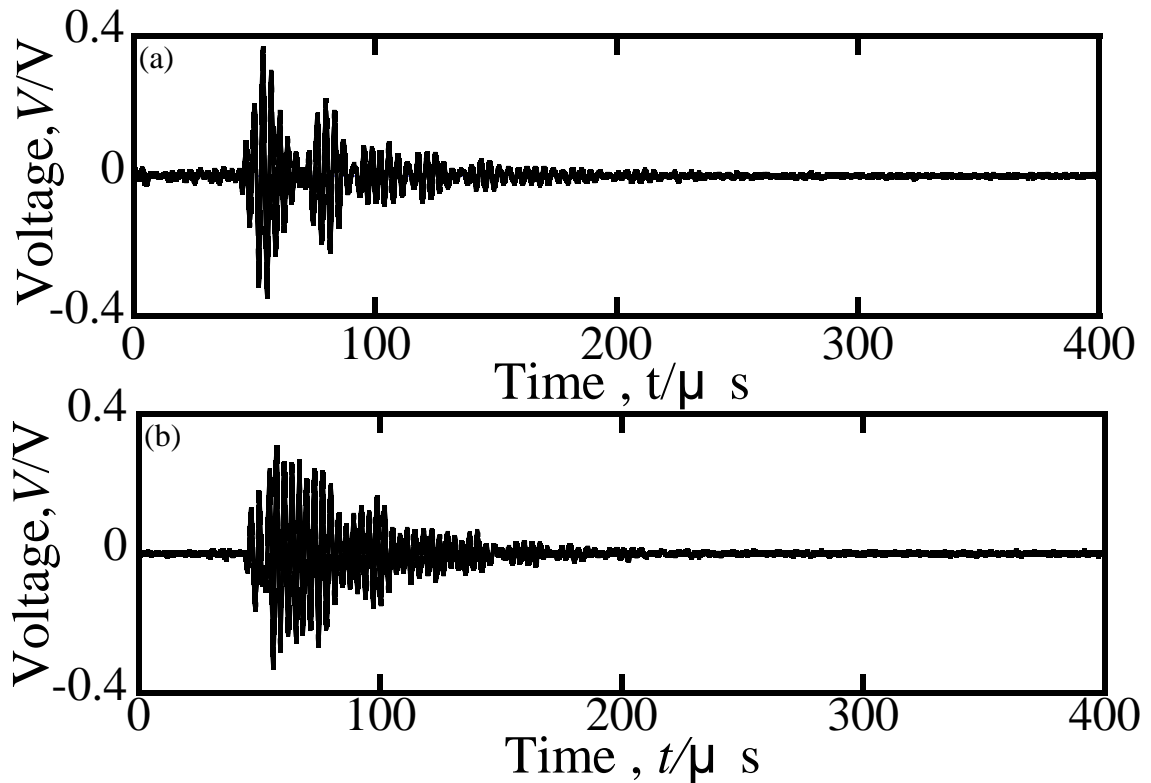


Fig. 3-6 Typical AE signals induced by O₂ gas generated on Pt electrode. These signals were randomly chosen, and the observed oftenness were (a) 92% and (b) 8%.

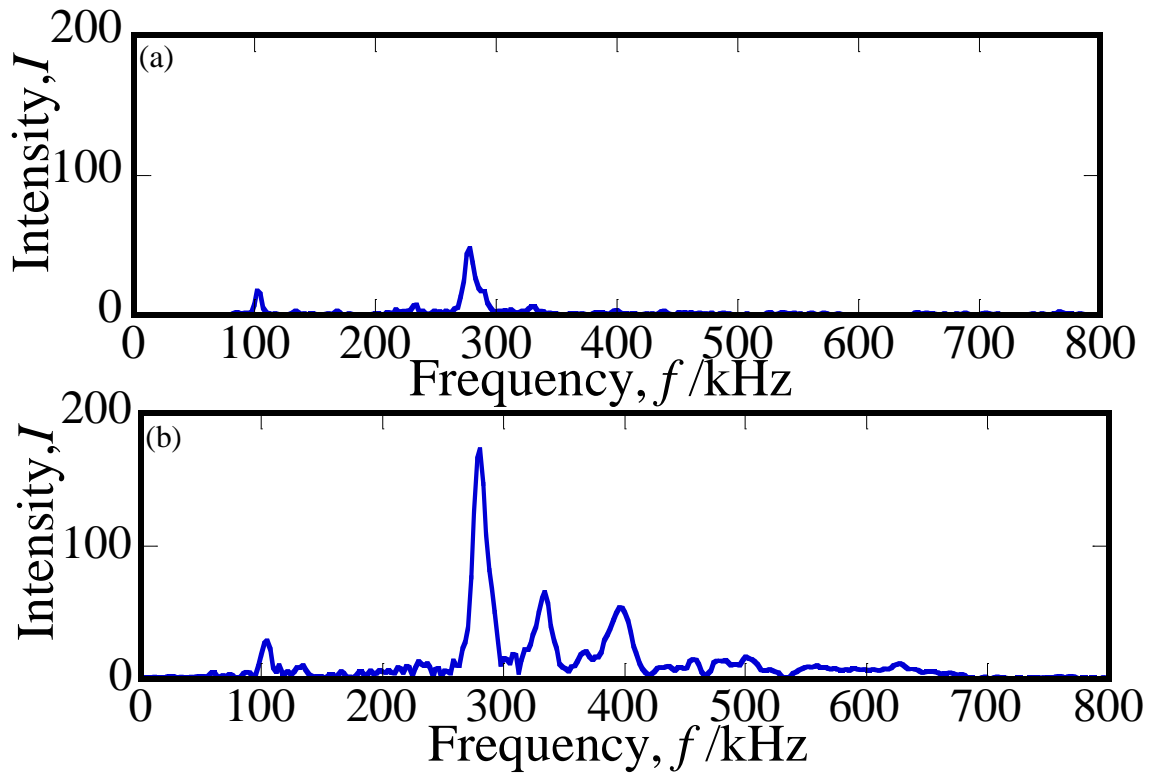


Fig. 3-7 Typical power spectrum induced by O₂ gas generated on Pt electrode.
Spectrum (a) and (b) correspond to the AE signal (a) and (b) in Fig. 6,
and observed oftenness were (a) 92% and (b) 8%, respectively.

H₂ gas generated on Pt electrode

Figure 3-8 (a) shows AE events histogram per 1 s as a function of decomposition voltage by H₂ gas generated on Pt electrode. The cumulative AE event is described in Fig. 3-8 (b). Figure 3-8 (c) shows current density versus applied voltage. As an experimental relation, N was given by exponential fitting of V . By using the same specimen, AE events behavior was same in the voltage repetitions, *i.e.*, in proportion to the amount of H₂ gas generated on the Pt electrode. AE event counts induced by H₂ gas was equal to around one third by O₂ gas as was shown in Fig. 3-5 (b).

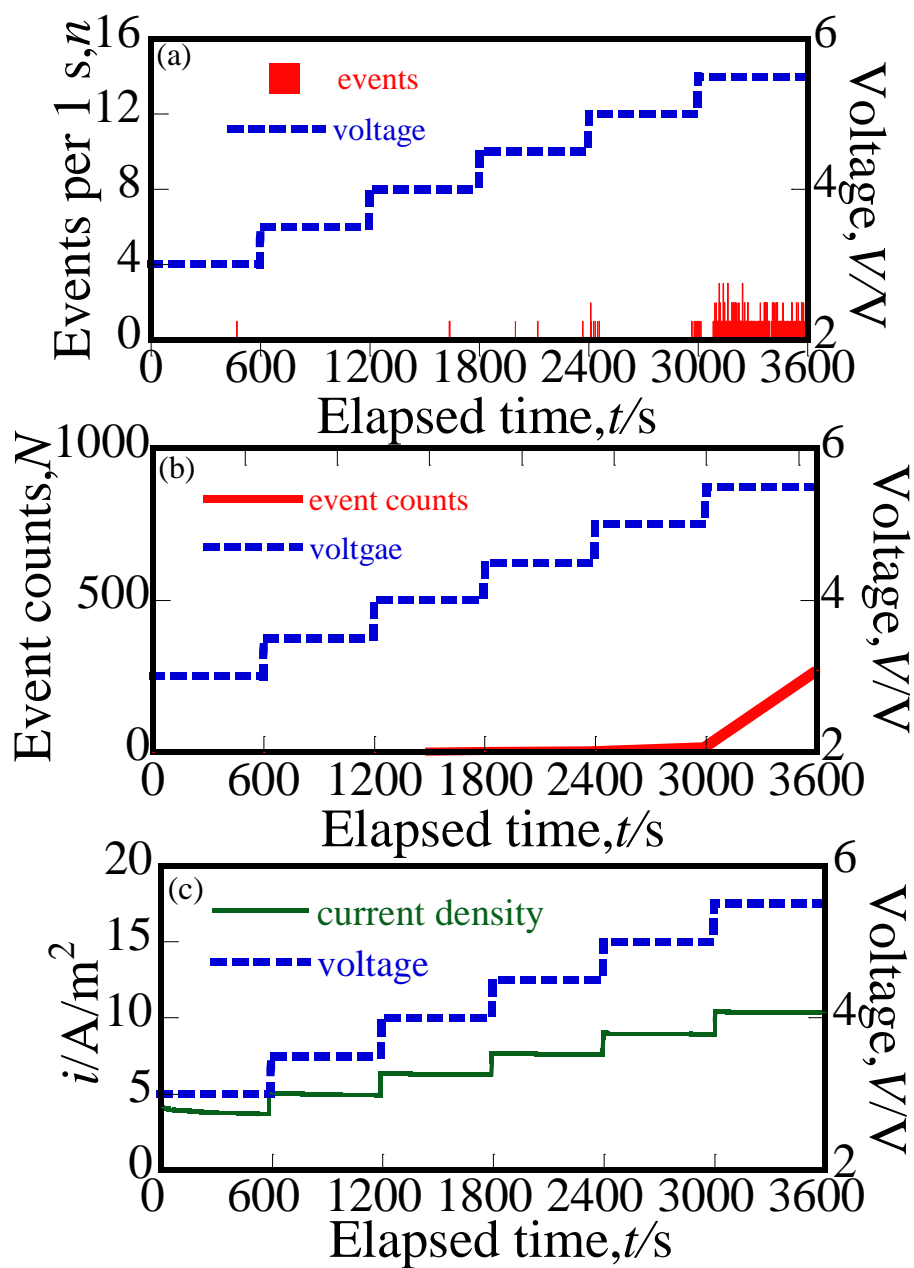


Fig. 3-8 AE events by H₂ gas generated on working Pt electrode as a function of decomposition voltage;
 (a) AE events per 1s, (b) cumulative AE event counts, (c) current density.

Figure 3-9 (a) and (b) show the typical AE signals by H₂ gas generated on Pt electrode, which were randomly chosen. Figure 3-10 (a) and (b) are the FFT spectrum of the corresponding signals, where the observed oftenness was around 90 % and 10 %, and the intensity at 280 kHz peak was 50 and 200, respectively. Accordingly, the feature of the AE power spectrum (a) of the H₂ gas generated on Pt was also induced by cavitation and the spectrum (b) was due to bubble burst.

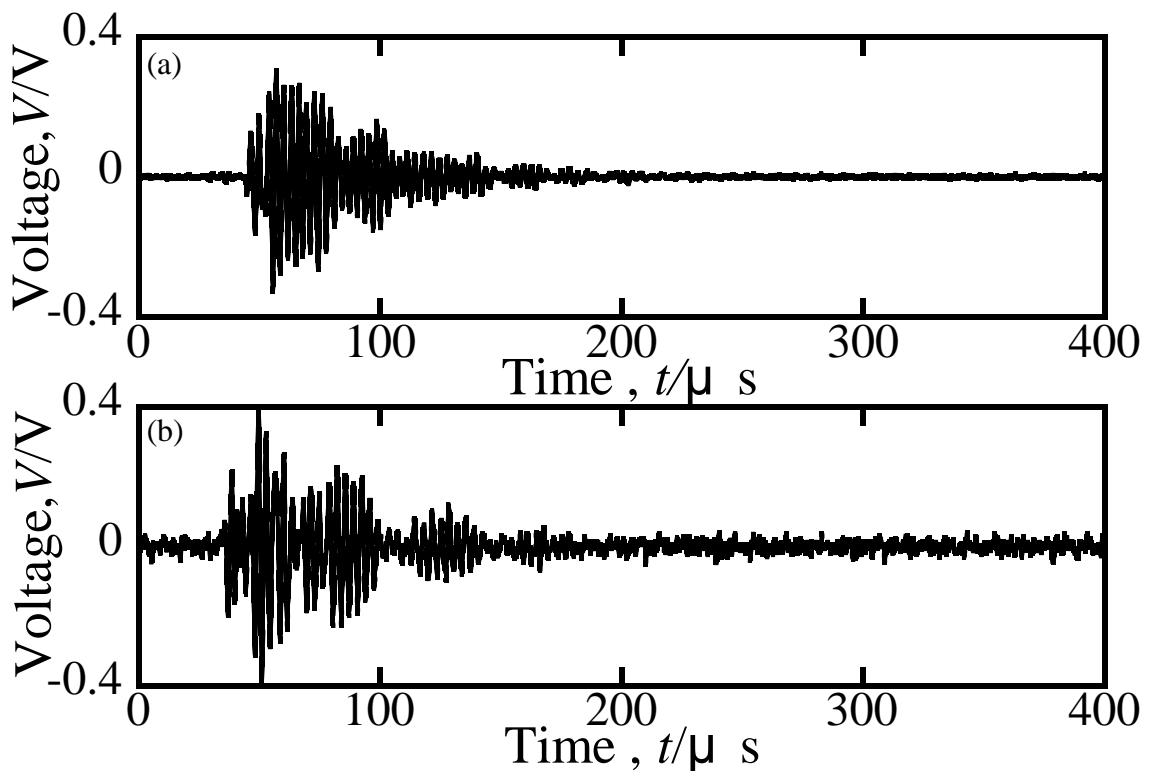


Fig. 3-9 Typical AE signals induced by H₂ gas generated on Pt electrode.

These signals were randomly chosen, and the observed oftenness were (a) 90% and (b) 10%.

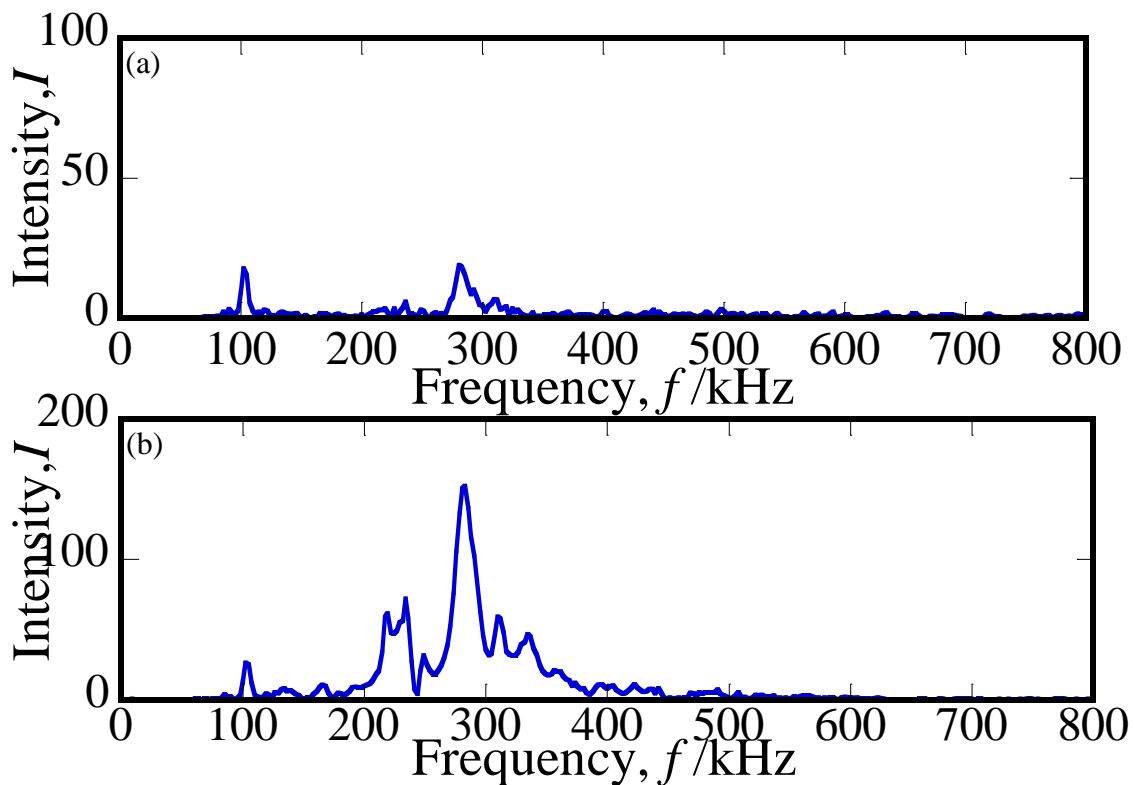


Fig. 3-10 Typical power spectrum induced by H₂ gas generated on Pt electrode.

Spectrum (a) and (b) correspond to the AE signal (a) and (b) in Fig. 3-9, and observed oftenness were (a) 90% and (b) 10%, respectively.

3.3.3 Experimental results on Pd electrode as present purpose

O₂ gas generated on Pd electrode

Figure 3-11 (a) shows AE events histogram per 1s as a function of decomposition voltage V by O₂ gas generated on Pd electrode. The cumulative AE event is described in Fig. 3-11 (b). Figure 3-11 (c) shows current density versus applied voltage. The event counts were 3776 induced by stepwise decomposition from 3 V to 5.5 V on the Pd, which was 4 times of 965 on Pt under the same decomposition condition from 3 V to 5.5 V as basic data. The event counts N was expressed by cubic polynomial of V as was mentioned in section 3.2.1.

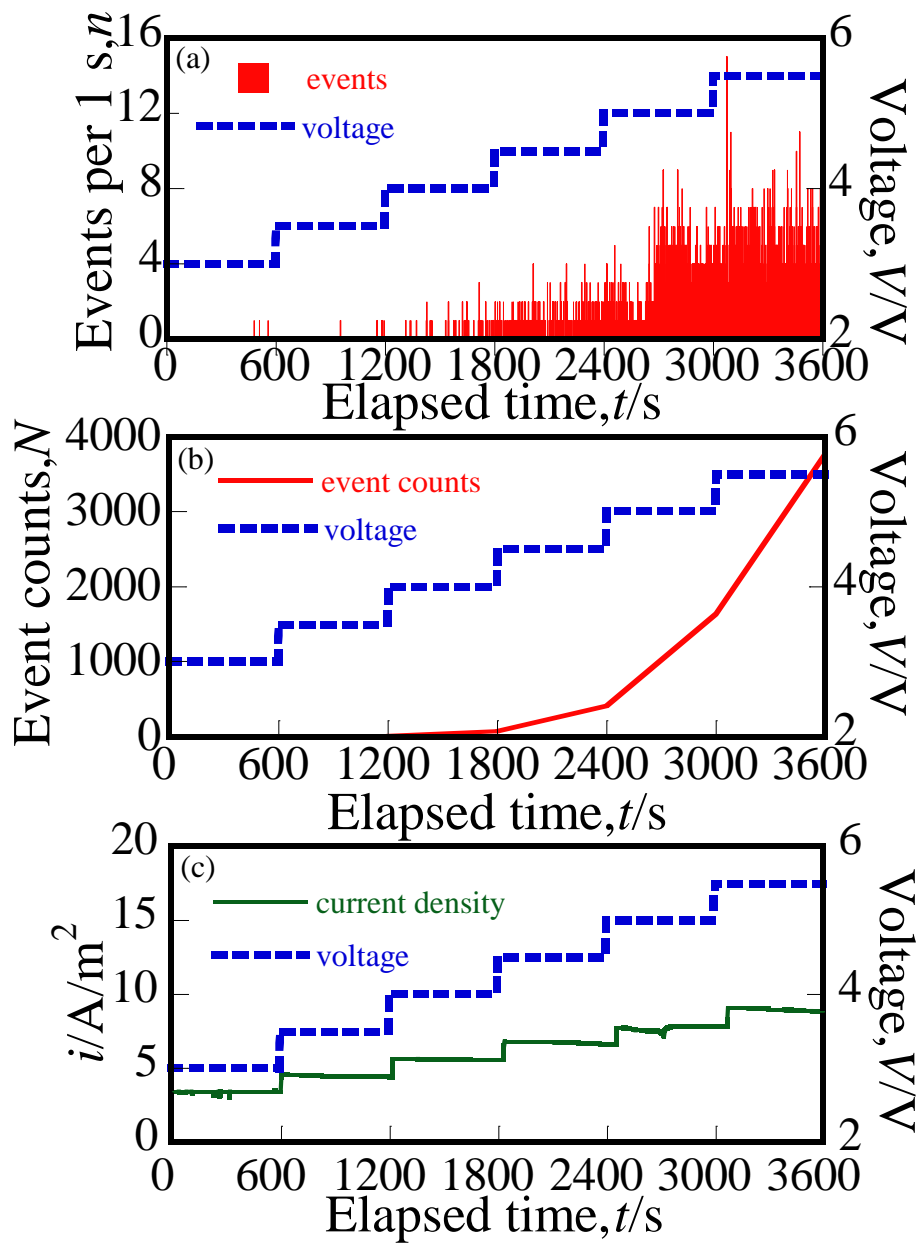


Fig. 3-11 AE events by O₂ gas generated working Pd electrode;

(a) AE events per 1s, (b) cumulative AE event counts, (c) current density.

Figure 3-12 shows the typical of AE signals by O₂ gas generated on Pd electrode. Figure 3-13 is the FFT spectrum of the corresponding signal. The power spectrum feature at 280 kHz indicates the cavitation induced signal. The bubble burst spectrum was not detected in this observation.

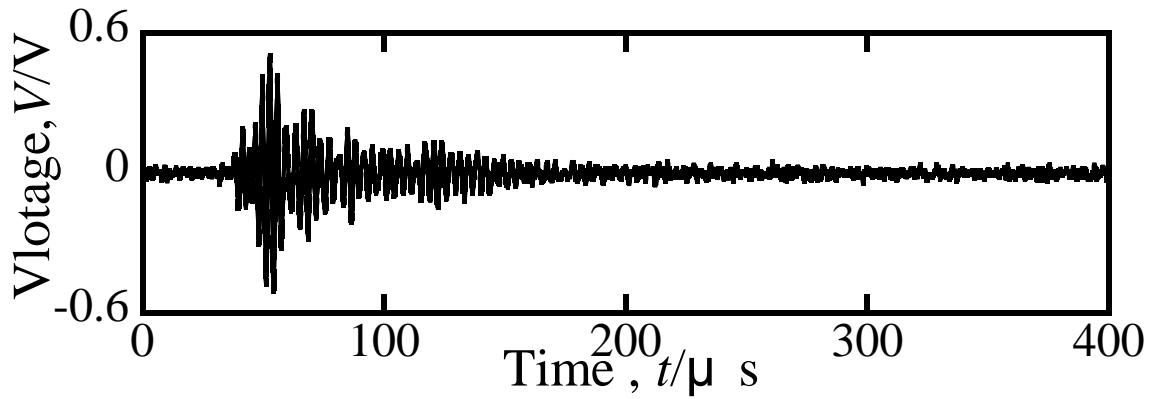


Fig. 3-12 Typical AE signal induced by O₂ gas generated on Pd.

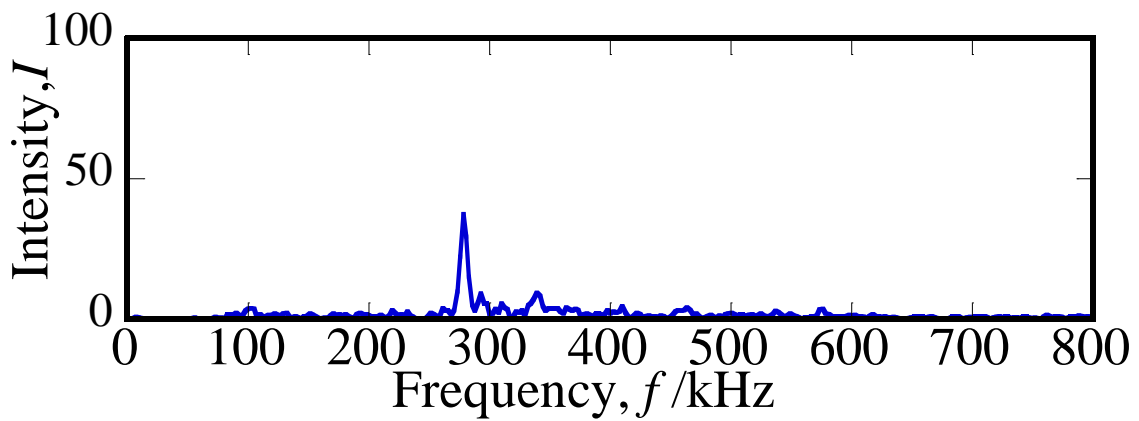


Fig. 3-13 Typical power spectrum induced by O₂ gas generated on Pd electrode.

AE measurement of Pd hydrogenation

Figure 3-14 shows AE events histogram as a function of decomposition voltage by H₂ gas on Pd electrode. The cumulative AE event is described in Fig. 3-14 (b). Figure 3-14 (c) shows current density versus voltage. As an experimental relation, N could not represent by simple exponential formula of V by cavitation due to the basic data of H₂ gas on Pt. The event counts at initial decomposition voltage of 3 V were occurred, which were induced by Pd hydride formation. The cumulative event counts from 3 V to 5.5 V were 1894 due to H₂ gas on Pd electrode, where the cumulative counts were 271 due to that on Pt. That is, the cumulative event counts by the Pd hydride formation should be 834 (=1894-1060). The counts of 1060 might be due to the cavitation by H₂ gas and be evaluated as $1060 \sim 3776_{(O_2 \text{ on Pd})} \times 271_{(H_2 \text{ on Pt})} / 965_{(O_2 \text{ on Pt})}$ by assuming that the relation on the event counts for O₂ and H₂ gas generated on Pt as was shown in section 3.2 should be adaptable for O₂ and H₂ gas generated on Pd.

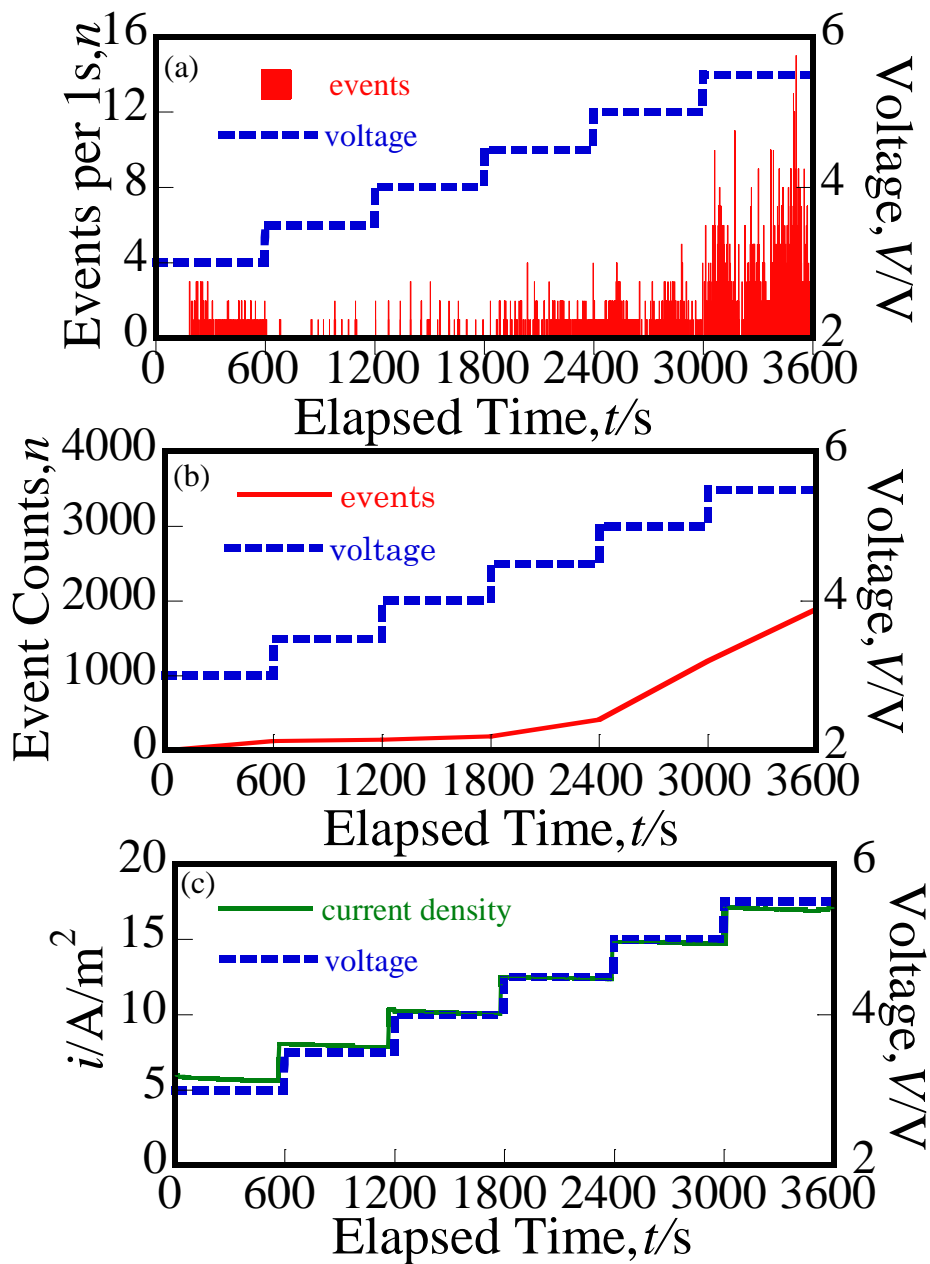


Fig. 3-14 AE events of the hydrogenation of Pd electrode;

(a) AE events per 1s, (b) cumulative AE event counts, (c) current density.

Figure 3-15 (a) shows the typical power spectrum of AE signal which was observed during the process of Pd hydride formation. The typical power spectrum induced by cavitation due to H₂ gas on Pd is given in Fig. 3-15 (b). The observed oftenness due to the hydride formation (a) and the cavitation (b) was around 30 % and 70 %. The oftenness of 30 % is fairly agreement with that of 44 % (=834/ (1060+834)) evaluated by cumulative event counts as was mentioned just above.

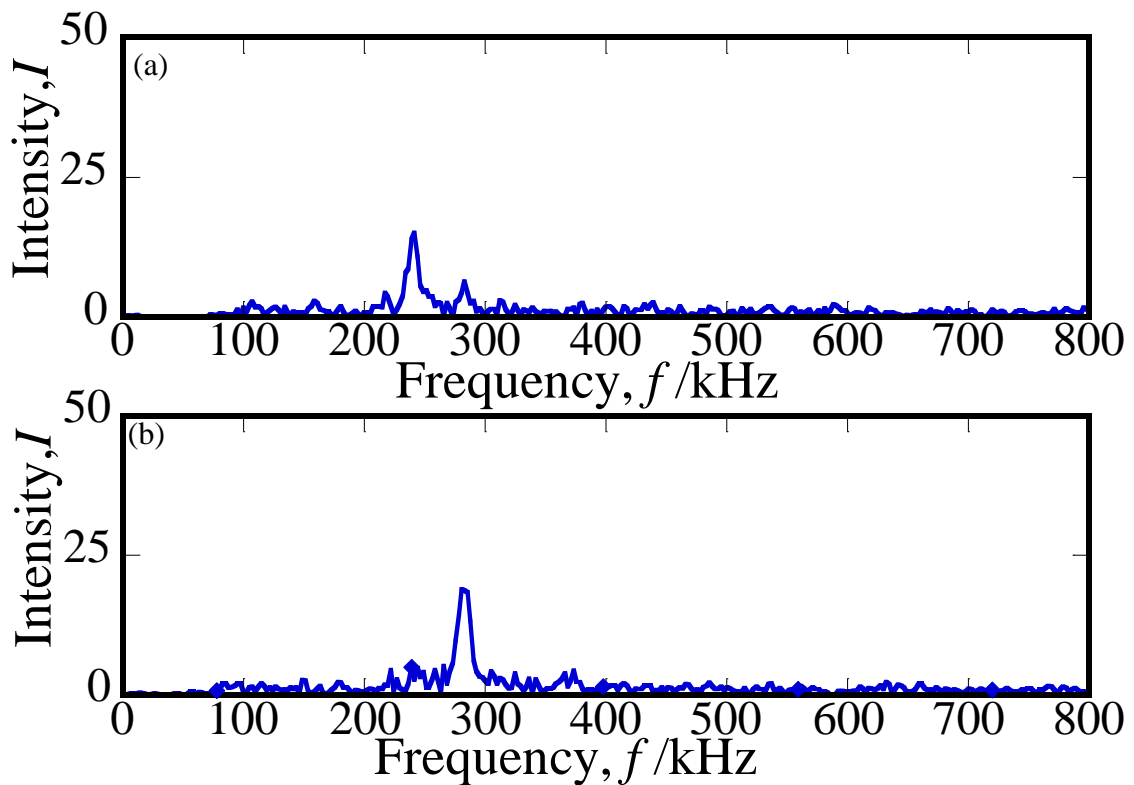


Fig. 3-15 Typical power spectrum of the hydrogenation of Pd electrode ;(a) power spectrum of Pd hydride formation, (b) power spectrum of H₂ gas cavitation.

3.4. Summary

In the present work, a hydrogenation process of Pd was studied by AE method with an electrochemical hydrogen charging technique. The characteristic of the AE power spectrum due to Pd hydride formation was around 250 kHz. In the previous paper³⁸⁾, the spectrum was evaluated as 250 kHz obtained using gas pressure AE cell. This means that the AE method with the electrochemical AE cell will be a powerful way to investigate the hydride formation mechanism because the high H₂ gas pressure condition can be easily provided by electrochemical applied voltage. Accordingly, we also propose that the partial dislocation of Pd lattice will play an important role in hydride formation as was mentioned in the previous paper³⁸⁾.

Chapter 4

CONCLUSIONS

Conclusions

In recent years, the concepts of saving energy, reducing pollution, protecting the environment, and developing long-term energy supply solutions were the main focus by the public attention. The world's current energy supply system which is mainly based on fossil fuels has become a matter of concern. The fuel cell technology and hydrogen as an alternative energy carrier are considered the ultimate goal of a secure energy supply and a clean environment. It is predicted that our country of China would have the highest share of hydrogen fuel cell vehicles in 2050 if their ambitious climate and energy security policies are adopted.

There are a lot of interests in the formation mechanism of metallic hydride. It has been known that the change of lattice energy of a transition metal by hydrogenation is interpreted in the terms of the lattice expansion and the change of Fermi level by our research group. That is, when a hydrogen atom is dissolved into an fcc metallic lattice, it occupies an interstitial octahedral (O) site and pushes aside metal atoms around its site as is recognized from the lattice expansion induced by hydrogenation. In a case of palladium-hydrogen (Pd-H) system, the solubility of hydrogen x increases with increasing pressure of H_2 gas P . The dissolution and diffusion measurements show that the penetration time of H in Pd sheet of $140\ \mu\text{m}$ is 67 s at 297 K. The occupied spaces of H are the interstitial O-sites of Pd. The number of O-sites in the fcc lattice is equal to that of the host Pd atoms. Palladium absorbs large amounts of hydrogen, up to $x = [H]/[Pd] = 1$, where the [B] means the number of B atoms. The concentration range of around $x < 0.01$ is called primary solid solution α phase, and $x > 0.6$ is hydride β phase at room temperature. Except for the regions is $\alpha+\beta$ two phases, *i.e.*, the spinodal decomposition region due to the long-range attractive H-H interaction. The volume

expansion of the host lattice in the α to β transition is $\Delta V = 1.57 \text{ cm}^3/\text{g-atom of H}$. The free energy of Pd-H system has been measured by thermal analysis and/or electrochemical methods and the formation mechanism of Pd hydride was interpreted on the basis of the lattice relaxation energy and the change of Fermi energy.

There are two kinds of hydrogenation methods, the gas pressure method and the electrochemical charging one. During hydride formation, host lattice will expand with hydrogen concentration. That is, lattice distortion energy will be increased by hydrogenation. Acoustic emission (AE) measurements are useful investigating method for dislocation motion caused by applied stress and/or lattice distortion. In this paper, we will propose an AE measurement method by using gas pressure technique and electrochemical charging technique in order to obtain the dynamical information of hydrogenation process of palladium.

The H_2 gas pressure method is a fundamental hydrogenation technique. The AE events were observed by using a new gas pressure cell. The experimental results by Ar gas pressurization showed as following: 1) AE events happened just at the times of pressurization, 2) the Kaiser effect was recognized in the re-pressurization process, 3) the power spectrum of AE signal by noble gas showed the fundamental signals of 250 kHz and 550 kHz, 4) the intensity of the power spectrum I_{250}^{aver} was 0.51 and that of I_{550}^{aver} was 0.49. In order to investigate the details of the hydrogenation process of Pd, the AE events were observed by H_2 re-pressurization of the third pressuring process. The experimental results were different from those of Ar gas as following: The AE events in the hydrogenation process of Pd happened "continually", the total amount of event counts in the hydrogenation process by H_2 gas was equal to about 1/10 of the

applied stress by Ar, in the early stage of primary H solid solution of Pd, the intensity of the power spectrum I_{250}^{aver} was 0.48 and that of I_{550}^{aver} was 0.52, in the hydride formation stage, the I_{250}^{aver} was increasing to 0.75 and I_{550}^{aver} was 0.25. The analysis with the power spectra of these AE signals was discussed by the dislocation theory. The slip dislocation energy of partial and perfect is evaluated by $U^{\text{partial}} : U^{\text{perfect}} = 1 : 3$ indicate that the AE 250 kHz and 550 kHz should depend on the partial dislocation and perfect one, respectively. Accordingly, we may propose the dynamical hydride formation mechanism with partial dislocation of Pd lattice.

In general, high H₂ gas pressure is required to form the hydride. On the other hand, electrochemical hydrogen charging technique is a powerful way of making the specimen absorbing hydrogen directly. The relation of pressure p with chemical potential Φ is given by equation of $p = p_0 \exp(2 \Delta\Phi/kT)$, where p_0 is standard pressure, Φ : over potential, k : Boltzmann constant and T : temperature. In the case of $T=298$ K and $\Phi=0.1$ V, the equivalent H₂ gas pressure is 240 MPa, and $\Phi=0.15$ V gives 10 GPa at the same temperature. The hydrogenation process of Pd was also studied by AE method with an electrochemical hydrogen charging technique. The characteristic of the AE power spectrum due to Pd hydride formation was around 250 kHz. The spectrum was evaluated as 250 kHz obtained using gas pressure AE cell. This means that the AE method with the electrochemical AE cell will be a powerful way to investigate the hydride formation mechanism because the high H₂ gas pressure condition can be easily provided by electrochemical applied voltage. Finally, we will propose that this research could contribute to the research and development of, for example, aluminum based hydride which crystal structure will change by hydrogenation.

References

Chapter 1

- 1) Bolat, P. and C. Thiel. INT J HYDROG ENERGY **39**(17)(2014) 8881-8897.
- 2) Cau, G., et al. Energy Conversion and Management **87**(0) (2014) 820-831.
- 3) García, P., et al. Journal of Power Sources **265**(0) (2014) 149-159.
- 4) García-Triviño, P., et al. INT J HYDROG ENERGY **39**(21) (2014) 10805-10816.
- 5) Janghorban Esfahani, I., et al. Renewable Energy **80**(0) (2015) 1-14.
- 6) Capellán-Pérez, I., et al. Energy **77**(0) (2014) 641-666.
- 7) Elías-Maxil, J. A., et al. Renewable and Sustainable Energy Reviews **30**(0) (2014) 808-820.
- 8) Hu, Y., et al. Energy **54**(0) (2013) 352-364.
- 9) Jiang, Z. and B. Lin. Energy **70**(0) (2014) 411-419.
- 10) Lin, B. and X. Ouyang. Energy Conversion and Management **82**(0) (2014) 124-134.
- 11) Shih, H.-Y. and C.-R. Liu. INT J HYDROG ENERGY **39**(27) (2014) 15103-15115.
- 12) Siqueiros, E., et al. Energy Procedia **61**(0) (2014) 1208-1212.
- 13) Smith, M. G. and J. Urpelainen. Environmental Science & Policy **25**(0) (2013) 127-137.
- 14) Gan, H., et al. Electrochemical Acta **174**(0) (2015) 164-171.
- 15) Gao, P., et al. Journal of Alloys and Compounds **539**(0) (2012) 90-96.
- 16) Rousselot, S., et al. Journal of Power Sources **195**(13) (2010) 4370-4374.
- 17) Sun, J., et al. Journal of Alloys and Compounds **641**(0) (2015) 148-154.
- 18) S. Harada: J. Phys. Soc. Jpn. **54** (1985) 168-174.
- 19) S. Harada: J. Phys. F: Met. Phys. **13** (1983) 607-617.

- 20) T. B. Flanagan and W. A. Oates: Ber. Bunsenges. Phys. Chem. **76** (1972) 706-714.
- 21) S. Harada: *Kotai Butsuri* (Solid State Physics) (Agne, Tokyo, ISSN0454-4544) **44** (2009) 53-60 [in Japanese].
- 22) Y. Fukai: *The Metal-Hydrogen System* (Springer Verlag, Berlin, 2005, ISBN 3540004947) Chap. 2.
- 23) E. Wicke and H. Brodowsky: *Hydrogen in Metals II* (Springer Verlag, Berlin, 1978) 73-155.
- 24) S. Harada and S. Tamaki: J. Phys. Soc. Jpn. **54** (1985) 1642-1647.
- 25) M. Onoe: *Acoustic Emission -Bases and Applications*, (Korona, Tokyo, 1976, BN01345670) [in Japanese] Chap. 1, 2, 3 and 4.
- 26) I. G. Scott: *Basic acoustic emission* (Gordon and Breach Science, Berlin, 1991, ISBN2881243525) Chap. 1, 2 and 3.
- 27) T. B. Flanagan and W. A. Oates: Ber. Bunsenges. Phys. Chem. **76** (1972) 706-714.
- Chapter 2**
- 28) S. Harada: *Kotai Butsuri* (Solid State Physics) (Agne, Tokyo, ISSN0454-4544) **44** (2009) 53-60 [in Japanese].
- 29) Y. Fukai: *The Metal-Hydrogen System* (Springer Verlag, Berlin, 2005, ISBN 3540004947) Chap. 2.
- 30) E. Wicke and H. Brodowsky: *Hydrogen in Metals II* (Springer Verlag, Berlin, 1978) 73-155.
- 31) S. Harada and S. Tamaki: J. Phys. Soc. Jpn. **54** (1985) 1642-1647.
- 32) S. Harada, T. Kasahara and S. Tamaki: J. Phys. Soc. Jpn. **54** (1985) 430-437.
- 33) M. Onoe: *Acoustic Emission -Bases and Applications* (Korona, Tokyo, 1976, BN01345670) [in Japanese] Chap. 3 and 4.

- 34) I. G. Scott: *Basic acoustic emission* (Gordon and Breach Science, Berlin, 1991, ISBN2881243525) Chap. 2 and 3.
- 35) Edited by T. Kishi, M. Ohtsu and S. Yuyama: *Acoustic Emission - Beyond the Millennium* (Elsevier, Amsterdam, 2000, ISBN 0080438512) 1-56.
- 36) P. Haasen: *Physikalische Metallkunde* (Springer-Verlag, Berlin, 1981) Chap. 11.
- 37) S. Harada, H. Tanaka, H. Araki and M. Kubota: *Mater. Trans.* **49** (2008) 2895-2898.

Chapter 3

- 38) S. Harada, T. Otake and J. Piao: *Mater. Trans.* **53** (2012) 1726-1731.
- 39) B. Assouli, A. Srhiri and H. Idrissi: *NDT and E Int.* **36** (2003) 117-126.
- 40) B. Assouli, F. Simescu, G. Debicki and H. Hidrissi: *NDT and E Int.* **38**(2005) 682-689.
- 41) S. Didier-Laurent, H. Idrissi and L. Rou e: *J. Power Sources* **179** (2008) 412–416.
- 42) S. Harada, T. Kasahara and S. Tamaki: *J. Phys. Soc. Jpn.* **54** (1985) 430-437.
- 43) M. Onoe: *Acoustic Emission -Bases and Applications*, (Korona, Tokyo, 1976, BN01345670) [in Japanese] Chap. 3 and 4.
- 44) I. G. Scott: *Basic acoustic emission* (Gordon and Breach Science, Berlin, 1991, ISBN2881243525) Chap. 2 and 3.
- 45) Y. Fukai: *The Metal-Hydrogen System* (1998, ISBN 4-7536-5608-X C3042) [in Japanese] Chap. 2 and 3.
- 46) S. Harada: *J. Phys. Soc. Jpn.* **68** (1999) 1746-1750.
- 47) M. Boinet, J. Bernard, M. Chatenet, F. Dalard and S. Maximovitch: *Electrochimica Acta* **55** (2010) 3454–3463.
- 48) H. Inoue, R. Tsuzuki, S. Nohara and C. Iwakura: *J. Alloys Compd.* **446–447** (2007) 681–686.

Acknowledgements

I would like to express the deepest gratitude first and foremost to Professor Shuji Harada, my supervisor, for his constant guidance in the writing of this dissertation, as well as during my whole master and doctoral period. His perfect-pursuing character, which makes the high quality of all the work be ensured, has been a goal for me to pursue. His deliberate mind, diligence and dedication to his work, and rigorous attitude of research motivate me to move forward all the times.

I would also like to extend my sincere acknowledgement to all the other supervisors, Professor Naoya Takeda, Professor Ryouzuke Shiina, Professor Nozomu Tsuboi, Dr. Takahiro Murakami and Dr. Zhiming Mao for their all aspects of instructive advices and useful suggestions on my dissertation and kind help to my daily research and study.

Furthermore, I am greatly indebted to every member in our laboratory, who has offered me invaluable help in the laboratory and daily life.

Last but not least, my thanks go to my beloved family for their thoughtful concern and great confidence in me through all these years.

APPENDIXS

Appendix 1

Figure A1 shows typical AE signals of the hydrogenation process of Pd around at 1800 s from starting in the H₂ gas on 0.6 MPa. Figure A2 shows typical AE signals of the hydrogenation process of Pd around at 3600 s from starting in the H₂ gas on 0.6 MPa. Figure A3 shows typical AE signals of the outgassing process in a minute unit from the Pd-H_{0.6} system at 6, 91 and 1180 min from the starting of the outgassing in a minute unit.

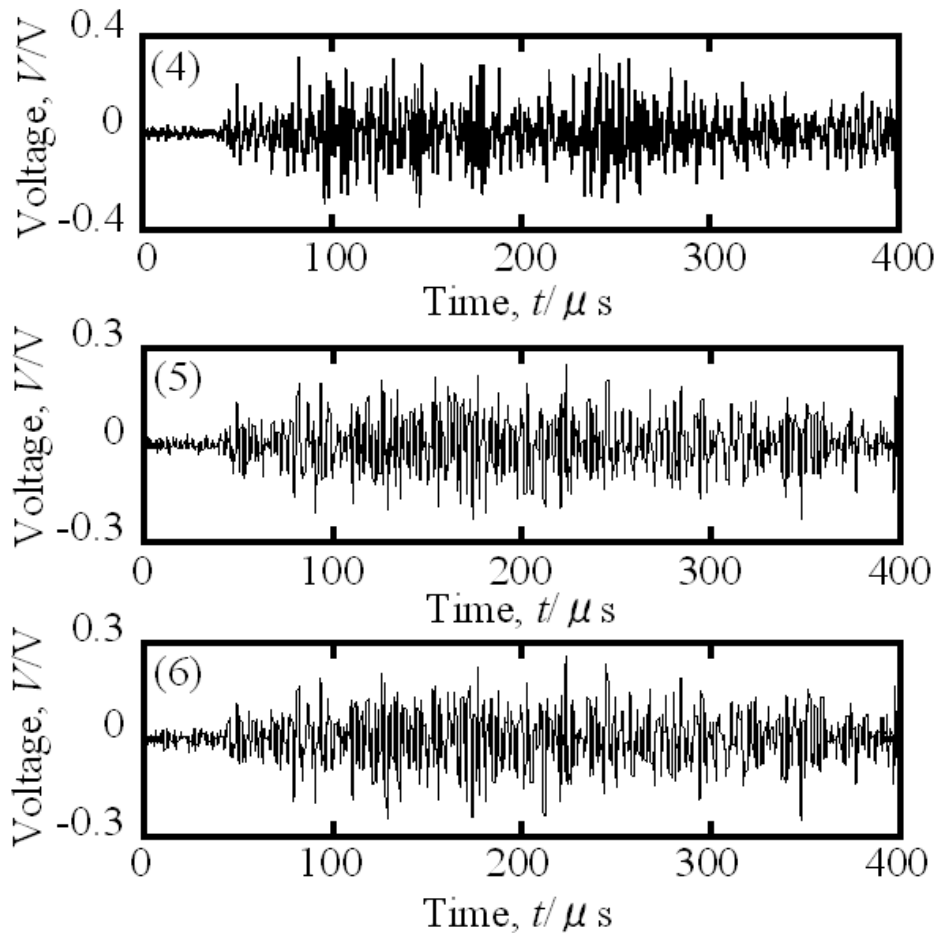


Fig. A1. Typical AE signals of Pd the hydrogenation process of Pd around at 1800 s from starting in the H₂ gas on 0.6 MPa.

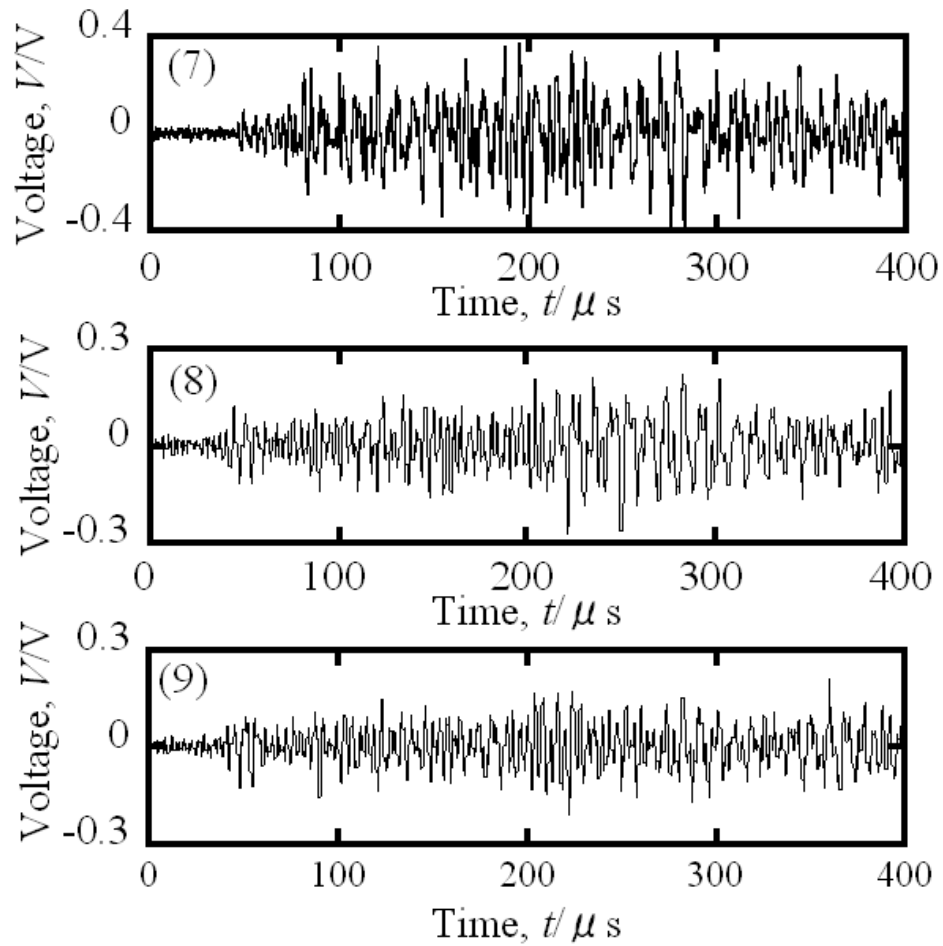


Fig. A2. Typical AE signals of Pd the hydrogenation process of Pd at around 3600 s from starting in the H_2 gas on 0.6 MPa.

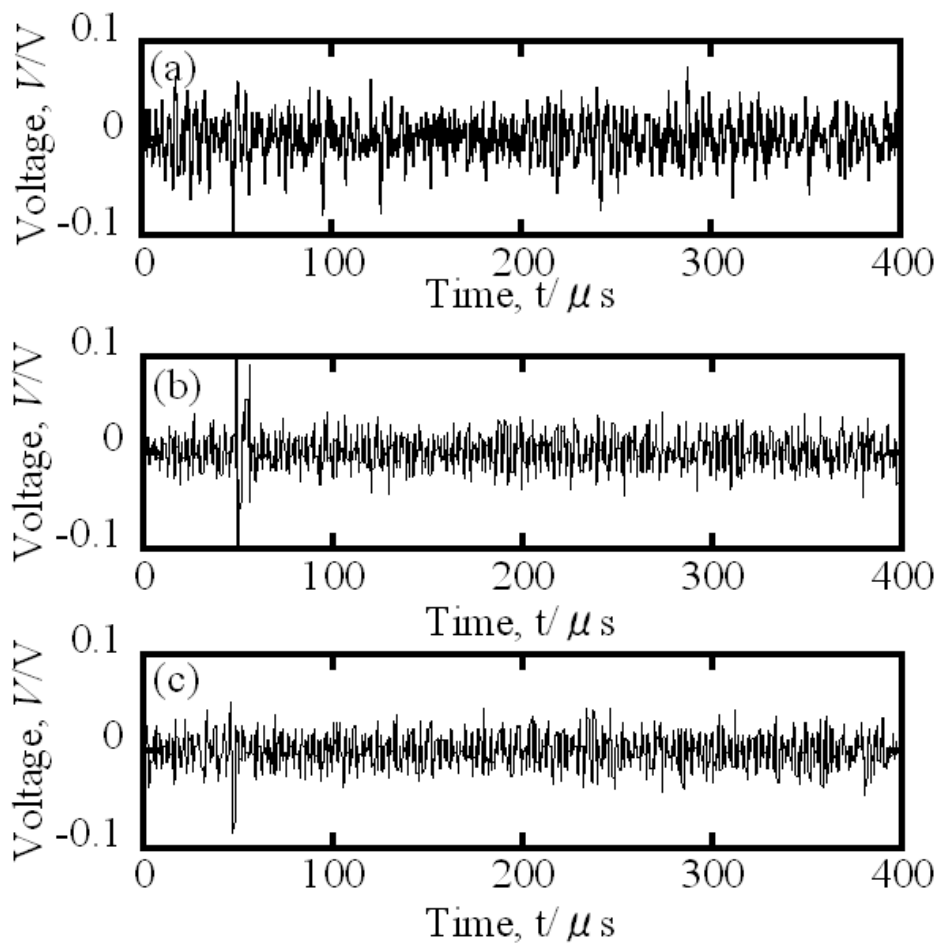


Fig. A3. Typical AE signals of the outgassing process of Pd-H system in a minute unit, (a) at 6 min, (b) 91 min and (c) 1180 min from the stating of the outgassing.

Appendix 2

The relation of pressure p with chemical potential Φ

Gibbs free energy with isothermal process equation of state is given by $dG = Vdp + \mu dN$. Characteristic equation of ideal gas is given by $V = kT / p$. By using Euler's relation of $dG = d(\mu n) = nd\mu + \mu dn$, partial free energy is written by

$\partial G / \partial N_{\text{H}} = \mu_{\text{H}}^{\text{H}_2} = (1/2)\mu_{\text{H}_2}^{\text{H}_2} = (1/2)kT \log p / p_0$. Accordingly, by using the relation⁶⁾ of

$$\Delta\mu = \mu_{\text{H}}^{\text{PdHx}} - \mu_{\text{H}}^{\text{H}_2} = -FE = -e\Delta\phi, \text{ we can obtain } p = p_0 \exp(2\Delta\phi / kT)$$